CHALMERS UNIVERSITY OF TECHNOLOGY
Chemical and Biological Engineering
Department of Forest Products and Chemical Engineering

Master Thesis

Modelling of reaction kinetics during black liquor pyrolysis

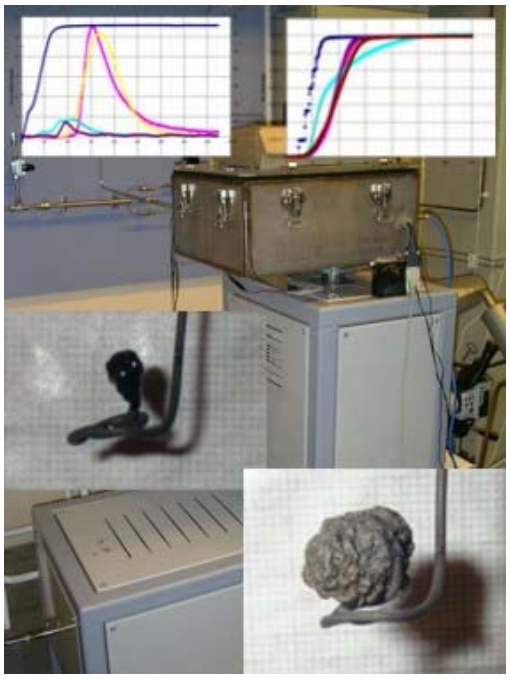

Stefan Heyne

Supervisors: Assistant professor Tobias Richards
PhD student Joko Wintoko
Examiner: Professor Hans Theliander

Gothenburg, February 2005

Summary

With this work the modelling of a single black liquor droplet has been investigated with focus on pyrolysis kinetics. An existing program has been extended to handle several different gas species, in particular CO, CO_2, CH_4 and SO_2. In addition, the heat transfer modelling in the program has been improved by implementing a relation that takes into account the internal thermal radiation. Experiments have been conducted, where a single black liquor droplet has been exposed to high temperatures in a nitrogen atmosphere. Online measurement of the release of these four gases in a temperature range of 275 to 400 °C, where the onset of pyrolysis reactions is to be expected, were recorded. Mass balances were set up to get more information about the dry mass loss during pyrolysis. The experimental data has been converted by the deconvolution method in order to have representative data for the gas release directly at the droplet location. This data was then used to adjust the kinetic parameters in the model used for the simulation. A set of two parallel reactions gave good fit for the evaluated temperatures of 375 and 400 °C. The kinetic parameters used for these two reactions are in the range of devolatilization parameters for coal but resulting in slower reaction kinetics for the observed temperature range. It was found that it is also possible to represent the gas release with one reaction only in the investigated temperature range.

Table of contents

Index of tables

Index of figures

Introduction

The kraft pulp process

The kraft process is the most common process used for pulping wood. In this process, Na_2S and NaOH are used as cooking chemicals. Due to environmental and economic reasons, these chemicals are recycled and recovered. The chemicals are part of the liquor cycle where they pass several stages to finally be reused as cooking chemicals. A schematic of the kraft process is given in figure 1.

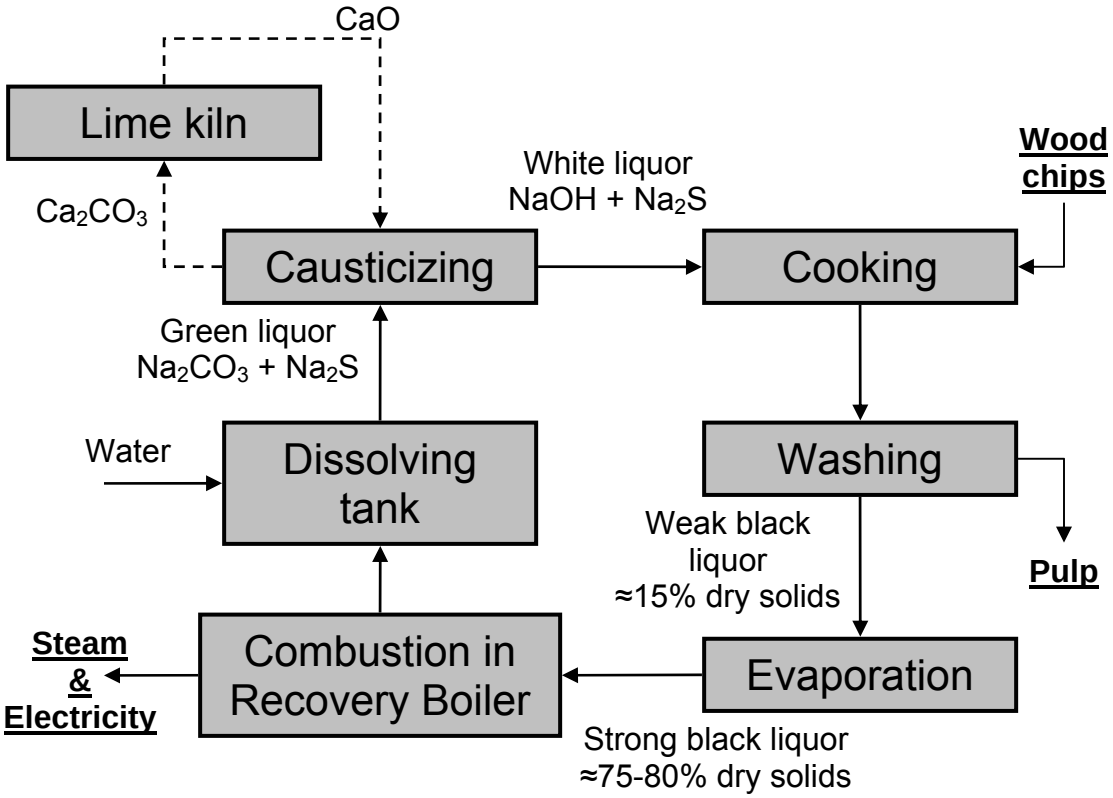

Figure 1: Schematic of the kraft pulping process (redrawn from [1])

After the first step – the cooking where lignin is separated from the wood chips – the formed pulp is separated and washed. From this washing process a so called weak black liquor is formed, having a dry content of about 15 %. It contains the

inorganic cooking chemicals, lignin as well as fibre material from the wood chips. The chemical cooking process does not only dissolve the lignin, but also parts of the wood fibres. This weak black liquor is, usually, evaporated in multistage evaporators to produce a strong black liquor with a dry content of about 75-80 %. Traditionally, the black liquor is then burned in a combustion unit, a recovery boiler, resulting in electricity and steam that is used to supply the plant with its need of energy. The smelt, resulting from the combustion process, contains the inorganic products from the cooking, mainly Na_2CO_3 and Na_2S, and is dissolved in water forming so called green liquor. This liquor is then causticized with CaO resulting in white liquor containing NaOH and Na_2S. By that step, the liquor cycle is closed and the white liquor can be used in the cooking process again. Another chemical loop is the calcium cycle. After the causticizing step, the calcium is in the form of $CaCO_3$ which is converted back to CaO again in a lime kiln. By these recycling efforts, the effluents from the pulping process are minimized. The aim or future vision for pulp and paper plants is to move towards a cyclic process using only the wood and solar energy as input and having no toxic emissions. This model must, of course, be seen on a larger scale than only the plant itself and has also to include recycling of paper. A schematic flow sheet of such an ecologically balanced process can be seen in figure 2.

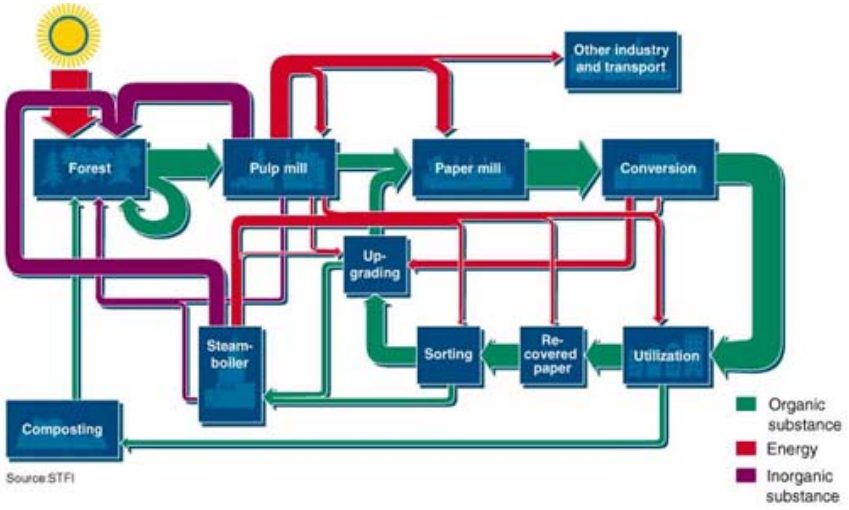

Figure 2: Vision on an ecologically balanced circuit [2]

Black liquor combustion and gasification

The part of the kraft process that this thesis work focuses on, is the black liquor stage. In nowadays practice, black liquor is combusted in a recovery boiler – the so called Tomlinson boiler - producing steam and electricity that, due to increasing efficiency, are sufficient to supply the pulping plant and may even result in a surplus of energy. Nevertheless, research is going on in the area of black liquor gasification because several advantages are expected when using this novel technology. The main difference between the two techniques is the available amount of oxygen for the conversion of the organic material in black liquor. In combustion, an excess of air is used whereas in gasification the oxygen level is restricted to values below 30% of the amount necessary for complete combustion. The drawbacks of the traditional setup of a Tomlison boiler combined with a back-pressure steam turbine CHP, to provide the mill with process steam and co-generated electricity, include the risk of explosion, as well as a low electric efficiency. The advantages of gasification might offer are an increased electric power output, higher operational safety as well as reduced emissions [3].

The different steps during black liquor gasification are: drying, pyrolysis and char gasification. These three phenomena occur at different temperature levels but may take place at the same time in a droplet if that droplet is thermally large. This leads to different temperatures inside the droplet, making it possible that the droplet is still drying in the centre whereas it already is pyrolysed or there is even char gasification taking place on the droplet's surface.

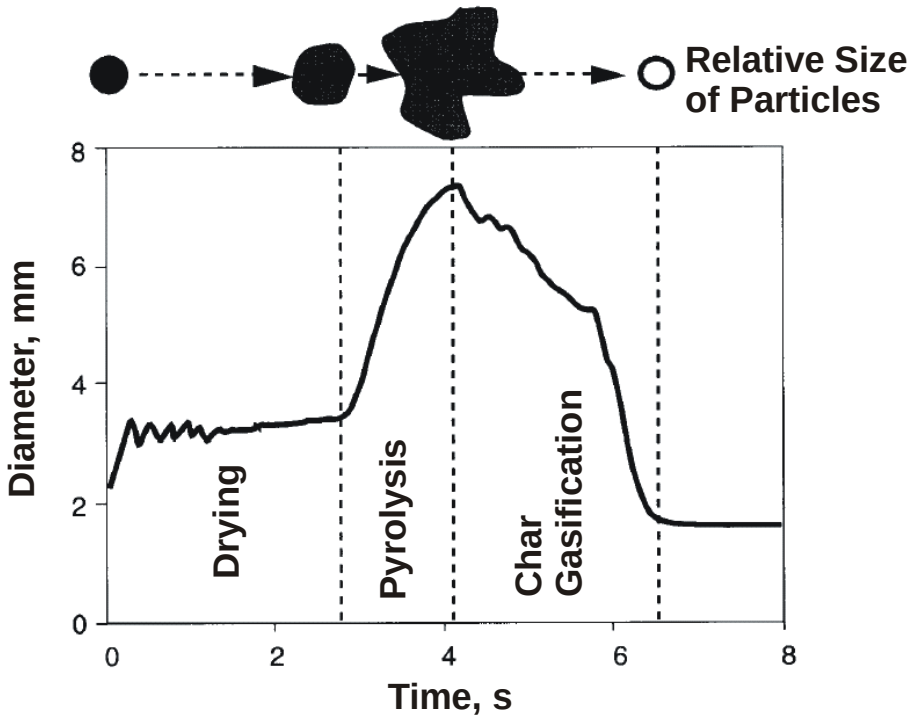

Figure 3: Stages of black liquor gasification (modified from [4])

Figure 3 shows the different stages and the schematic droplet swelling during the gasification process. The focus of this thesis is on the pyrolysis part. It is possible to simulate the process with a mathematical model and the goal here is to improve the kinetic parameters in order to get a better representation of the gas release during the pyrolysis process.

Pyrolysis kinetics

As the focus is on the improvement of the pyrolysis kinetics during black liquor a literature review on available data for kinetics of biomass pyrolysis was performed. In table 1 an overview of the found parameters and models is given.

Table 1: Kinetic models and parameters for pyrolysis

Material	Ex-perimental conditions	Model	Parameters	Source
Cellulose	T-range: 300-325 °C	Simple rate law	$A = 2.86 \cdot 10^{7}\ s^{-1}$ $E = 227$ kJ/mol	Antal et al [5]
Cellulose	T-range: 200-900 °C	Simple rate law	$A = 4.7 \cdot 10^{12}\ s^{-1}$ $E = 182.7$ kJ/mol	Cordero et al. [6]
Kraft lignin from eucalyptus	T-range: 500-900 °C	Simple rate law with temperature dependent parameters	$A = \exp[14.77 + 0.0208 \cdot (T - 273)]\ s^{-1}$ $E = 52.64 + 0.173 \cdot (T\text{-}273)$ kJ/mol	Caballero et al. [7]
Kraft lignin from eucalyptus	T-range: 200-900 °C	Simple rate law	$A = 0.655\ s^{-1}$ $E = 36.7$ kJ/mol	Cordero et al [6]
Kraft lignin	T-range: 227 – 503 °C	Simple rate law	$A = 3.3 \cdot 10^{7} - 1.84 \cdot 10^{9}\ s^{-1}$ $E = 80 - 158$ kJ/mol	Ferdous et al. [8]
Eucalyptus sawdust	Heating rate 5 °C/min	Two-stage overall reaction approach	$A_1 = 1.14 \cdot 10^{6}\ s^{-1}$ $E_1 = 101.8$ kJ/mol $A_2 = 2.07 \cdot 10\text{-}3\ s^{-1}$ $E_2 = 12.5$ kJ/mol	Cordero et al. [6]
Coal	T-range: 1500-2000 °C	Two reactions	$A1 = 3.70 \cdot 10^{5}\ s^{-1}$ E1 = 73.6 kJ/mol $A2 = 1.46 \cdot 10^{13}\ s^{-1}$ E2 = 251 J/mol	Ubhayakar et al. [9]

The parameters differ quite a lot for the different studies, even for the same material. This is mainly due to differences in the experimental methods and the resulting influence on the parameters, as it is practically impossible to obtain intrinsic parameters for a biomass material because there are several reactions taking place that are represented by only one or two reactions.

Former work on black liquor droplet simulation

There has already been many modelling work performed on the combustion of a single black liquor particle. The models can be divided into two main categories: models assuming an isothermal droplet and non-isothermal particle models. Assuming an isothermal droplet simplifies the calculations a lot but also can be a source of significant errors.

As one of the first isothermal models, Merriam [10] developed a computer model for a kraft recovery boiler. For the single droplet model, linear swelling of the droplet was assumed and devolatilization and char burning models for coal were directly applied for black liquor. Although this model could not describe the processes perfectly it was the basis for future modelling of black liquor furnaces. Shick [11] extended Merriam's model including the effect of a change in particle size on the droplet's trajectory in the furnace. The rate of devolatilization was modelled as a function of the gas temperature. The char combustion was based on an empirical equation not giving perfect match with black liquor char combustion rate. Kulas [12] proposed a single particle combustion model with drying and devolatilization being assumed to be heat transfer controlled processes. The char burning was assumed to take place only on the droplet surface, what probably is a too extreme simplification as black liquor is very porous during combustion. Frederick [13] developed a model including a simple thermal resistance model for the intra-particle heat-transfer and can therefore be defined as a transition to non-isothermal models. Drying took place at the boiling point and devolatilization at a distinct temperature between ignition and final temperature. Fredericks model was further developed by Thunman [14] refining the char conversion process considering H_2O and CO_2 gasification, direct O_2 gasification as well as sulphide/sulphate cycle by kinetic expressions.

Non-isothermal models have been presented by e.g. Harper [15] who divided each particle in 3 spherical concentric layers and solved the energy balances for all these sections to predict the rate of devolatilization and the sulphur release. No internal thermal radiation was included in the modelling of heat transfer. Mass

transfer was not considered and drying was assumed to take place at 150 °C. Manninen and Vakkilainen [16] developed a model combining the work of Frederick and Harper. Initial drying took place as an evaporating droplet. When a certain solids content is reached, ignition takes place and the non-isothermal model of Harper is used. During drying and devolatilization, mass transfer was not considered. Saastamoinen et al. [17] applied an earlier developed combustion model for wood particles assuming simultaneous drying and devolatilization to black liquor combustion. Another very similar model was presented by Verril et al. [18]. Devolatilization was described by three parallel reactions resulting in a temperature dependent product yield. An overview and more detailed summary of all these models on black liquor combustion can be found in Järvinen [1].

Simulation part

Description of the existing program

The program, written in MATLAB, calculates the time dependent swelling behaviour and gas release during drying and pyrolysis of a single spherical black liquor droplet. The simulation time is defined in seconds that are further divided in time steps per second. The more time steps one chooses the higher the calculation effort and risk for numerical errors is but at the same time the assumption of constant conditions during one time step is better fulfilled. The ideal case would be represented by an infinite number of time steps, what is not possible, of course.

The droplet is divided into sections for the calculation and a certain number of small bubbles are assumed to be inside the droplet taking up void volume and representing an initial porosity. The sectioning of the droplet is first done by defining radial points as centre of each section that all have the same distance from each other. In the next step, the intersection radii - defining the exchange area for mass and energy flow between the different sections of the droplet - are calculated to divide up the volume between to centre points equally. Then, the volume of each section can be determined and the centre points are recalculated to again divide each section into to equal volumetric parts. Finally, the number of the bubbles in each section is set and the bubble radius is determined with the help of the initial porosity. The thermal properties, as well as the composition of each section, are set to the starting conditions. The initial temperature and pressure of the droplet are assumed to correspond to ambient conditions (T_0 = *300 K*, P_0 = *101325 Pa*).

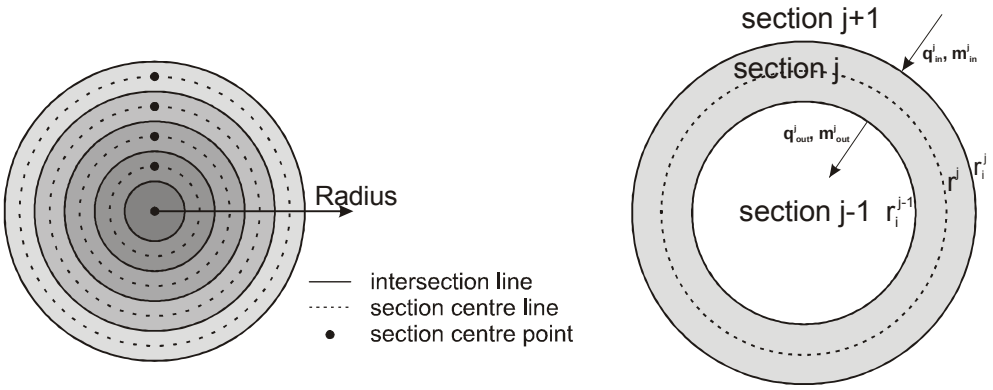

Figure 4: Droplet segments

For each time step, the program is running a loop where the pressure in each section is guessed based on previous values. Inside that loop – starting from the innermost section and "moving" outwards - the flow of mass and energy between the sections, the evaporation of water and the pyrolysis for all sections are calculated. These changes then result in a new pressure and temperature that is used as input for the pressure guess in the beginning of the loop. The loop is repeated until the maximum difference in the guessed pressure and the new one, obtained from the calculations in the loop, is less than a set level (0.2 percent for instance) for all the sections. The reactor temperature and pressure are assumed to be constant during the whole process. The general flow sheet for the program can be seen in figure 5. The different calculations in the loop are explained more in detail in the specific sections.

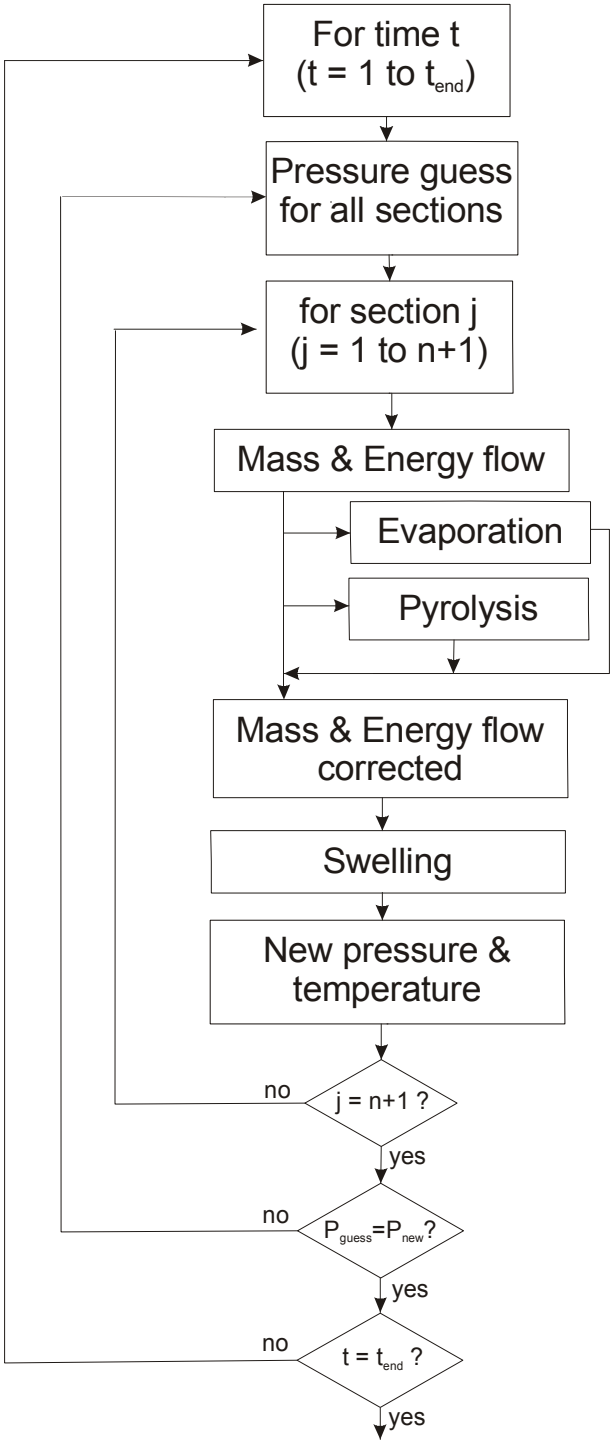

Figure 5: General program flow sheet

Mass and energy flow

First, for a better understanding, the definition of transport directions and the intersectional areas for the mass and energy exchange in the program are explained.

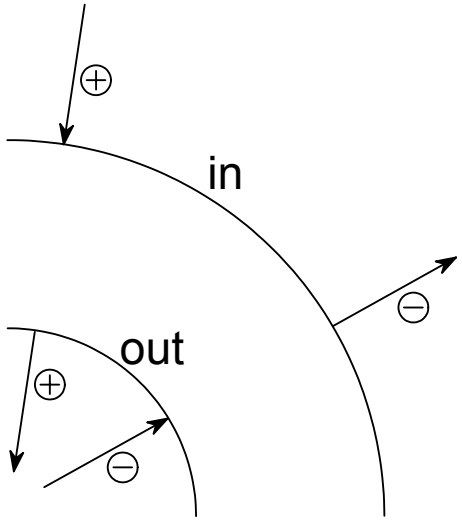

Figure 6: Definition of transport directions and intersectional areas

A positive transport means transport in opposite radial direction respectively in direction of the droplet's centre whereas a negative transport is describing transport of mass or energy in radial direction, meaning in direction to the droplet surface or leaving it in case of the outermost section. This implies that the gas flow at the inner boundary of section j $m_{G,out}^{j}$ is equal to $m_{G,in}^{j-1}$ of the previous section. A change of sign is not necessary as the direction is already included in m_G, representing a vector. The same principle applies for the energy flow.

According to Darcy's law, the flow through porous media can be described as:

$$\dot{m} = -\frac{K}{\mu} \cdot A \cdot \rho \cdot \Delta P \qquad (1)$$

with $\dot{m}$ being the mass flow [kg/s], K the Darcy constant [m], μ the dynamic viscosity [Pa·s], A the cross-sectional area [m^2], ρ the density [kg/m^3] and ΔP the pressure difference [Pa].

In the program, the mass change for each time step is calculated. This means that the Darcy equation has to be divided by the time step in order to obtain the accumulated mass in a section for one time step. The density is calculated by the ideal gas law using the average molar mass of the gas mixture. The area A, that the flow is related to, is the intersectional area between the different sections or the outer droplet area in case of the outermost section. The calculations in the program are done as follows:

$$m_{G,in} = \left(-\frac{K}{\mu} \cdot 4 \cdot \pi \cdot r_i^2 \cdot \frac{\phi^3}{(1-\phi)^2} \cdot \frac{P \cdot M}{R \cdot T} \Delta P \right) \Big/ tstep \qquad (2)$$

where r_i is the intersection radius for the inner sections and the droplet radius for the outmost section, ϕ is the porosity [-], P the pressure [Pa] and T the temperature [K] of the section under consideration. ΔP is the pressure difference between the section under consideration and the next section in radial direction. Looking at the outmost section, it is the difference between the pressure inside that section and the ambient pressure in the reactor. The molar mass M is calculated as the average molar mass of the gas mixture in the corresponding section. In case of gases flowing in direction of the center of the droplet, a small error is introduced because the exact composition of the outward section is only now for the previous time step. But this error can be neglected, considering that the time steps are very small and the change in the sections is relatively small. Besides, the case that gas is flowing in direction to the centre of the droplet is very rare as the pressure gradient nearly always is in radial direction to the droplets surface. The porosity in equation (2) is included in order to take into account the change of the Darcy constant with the changing structure of the droplet solid material during swelling. This correlation is derived from a more advanced model for permeability based on particle size, porosity and flow rate [19].

Contributions to the energy flow between sections can be: conduction, convection, radiation and the latent heat in the gas flow between the sections. Considering the outmost section, the energy accumulation can be related to the

convective and radiative heat transfer from the surroundings and the energy content of the gas coming into, respectively, leaving the droplet.

$$q_{in} = \frac{4 \cdot \pi \cdot r^2}{tstep} \cdot \left[\underbrace{h \cdot \left(T_{surr} - T\right)}_{\text{convection}} + \underbrace{\varepsilon \cdot \sigma \cdot \left(T_{surr}^4 - T^4\right)}_{\text{radiation}} \right] + \underbrace{m_{G,in} \cdot c_{p,G} \cdot \left(T - 273.15K\right)}_{\text{due to gas flow}} \qquad (3)$$

with r being the droplet radius, T_{surr} the temperature in the reactor [K], T the droplet temperature in that section [K], ε the emissivity factor [-], σ the Stefan-Boltzman constant [W/(m^2·K^4)] and $c_{p,G}$ the heat capacity of the gas flow [J/(kg·K)].

For the inner sections q_{in} is set up from only a term for the conduction and the change in energy due to the gas flow.

$$q_{in} = \frac{4 \cdot \pi \cdot r_i}{tstep} \cdot k \cdot \frac{\Delta T}{\Delta r} + m_{G,in} \cdot c_{p,G} \cdot \left(T - 273.15K\right) \qquad (4)$$

where r_i is the intersection radius [m] between the section under consideration and the next section in outward radial direction, ΔT the temperature difference [K] between the outer section and the actual section and Δr the distance between the radii [m], respectively.

In the next step, the accumulation of mass and energy for each section is calculated. A preliminary value for the mass increase of gas in the actual section can be estimated

$$m_{G,acc} = m_{G,in} - m_{G,out} \qquad (5)$$

The value of $m_{G,acc}$ can still be changed during the calculations depending on the release of gases in the section itself due to evaporation or pyrolysis. For the inner section the change in mass $m_{G,out}$ is set equal to zero. Gases transported at the inner boundary of a section are indexed “out” whereas transport at the outer section is referred to as “in” in the index. Therefore the transport at the inner boundary in the innermost section – the centre of the droplet - can be set to zero.

In a similar way, a preliminary value for the energy accumulation is estimated.

$$q_{acc} = q_{in} - q_{out}\,. \qquad (6)$$

This value will change in case any evaporation or pyrolysis occurs in the section under consideration.

Before starting the calculations for evaporation and pyrolysis, the necessary data for the calculations – namely dry content, heat capacities and boiling point – are obtained. The dry content of each section is calculated as:

$$DC = \frac{m_S}{m_S + m_W} \tag{7}$$

For the calculation of the heat capacities of the solid, the water and the excess heat capacity of black liquor in [J/(kg·K)] a separate function is defined using the following formula:

$$C_{p,S} = 1684 + 4.47 \cdot \left(T - 273.15K\right) \tag{8}$$

$$C_{p,W} = 4180 \tag{9}$$

$$C_{p,E} = \left(4930 - 29 \cdot \left(T - 273.15K\right)\right) \cdot \left(1 - DC\right) \cdot DC^{3.2} \tag{10}$$

The excess heat capacity accounts for the changes in black liquor heat capacity above 50 w-% dry content where a linear mixing rule for water and black liquor solids does not apply anymore [4]. With the help of these three values it is possible to calculate the overall heat capacity of black liquor depending both on temperature and dry content for black liquor.

$$C_{p,BL} = \left(1 - DC\right) \cdot C_{p,W} + DC \cdot C_{p,S} + C_{p,E} \tag{11}$$

It has to be considered that this correlation has been derived from data at temperatures below 100 °C and the accuracy for higher temperatures may be low.

The boiling point calculation is based on the correlation

$$T_{boil} = 373K + 50 \cdot DC^{2.74} + 101.6 \cdot P^{0.2487} - 101.39 \tag{12}$$

where the last two terms represent a correlation for boiling point raise data. The pressure *P* has to be given in [bar]. The correlation was initially based on a correlation atmospheric pressure for solid contents above 50 w-% given as [4]

$$T_{boil} = 373K + 50 \cdot DC^{2.74} \tag{13}$$

but as the pressure inside the droplet during the calculations may increase up to several bar, a pressure dependence was implemented based on the increase in boiling point for pure water with higher pressure [20].

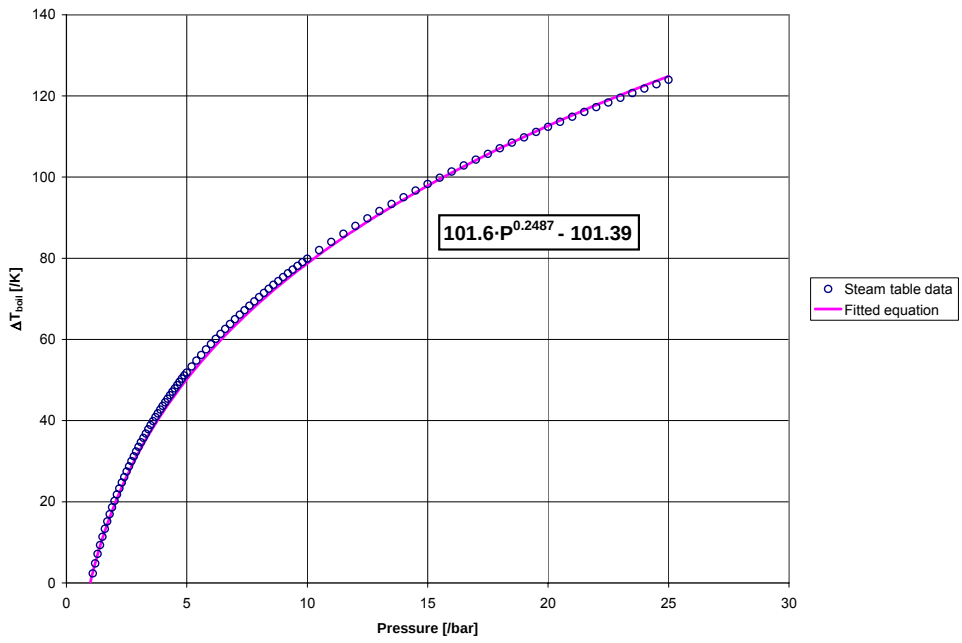

Figure 7: Increase in boiling point for pure water with higher pressure based on [20]

The two effects were added to give equation (12). There are more accurate ways of estimating the boiling point rise for black liquor available [4], but these require extensive and accurate measurements of heat capacity and normal boiling point over the range of solid contents of interest. As this data was not available equation (12) had to be used.

Drying and Pyrolysis

Based on the necessary data, the program calculates the temperature in the actual section and, depending on it, either of the following three options is chosen:

- No drying or pyrolysis
- Only drying
- Only pyrolysis

It is not possible that drying and pyrolysis occur simultaneously in the same section. This represents a simplification, but should be acceptable because these two phenomena occur at different temperatures. Of course, it is possible that in

the whole droplet these two phenomena may occur at the same time, i.e. when the outer sections have reached high enough temperature for the pyrolysis reactions while drying still occurs in the inner sections.

First, the program compares the actual temperature with the boiling point for water and if there is any water left in the section to evaporate. If the temperature is too low, the calculation part for drying and pyrolysis is finished for that section. If the temperature is higher than the boiling point and there is water left in the section, it is first assumed that all water in the section is evaporated. This step is included to decrease the calculation time. To check if the assumption is correct, the energy accumulation, q_{acc}, is reduced with the necessary amount to evaporate all the water and then the new temperature is calculated using equations 14 and 15.

$$q_{acc,new} = q_{acc} - m_w \cdot \Delta H_{evap} \tag{14}$$

$$T_{new} = T + \frac{q_{acc,new}}{m_S \cdot C_{p,S} + m_W \cdot C_{p,W} + m_G \cdot C_{p,G}} \tag{15}$$

The mass of water in equation (15), m_w, is zero in this case and the amount of gases is increased by the evaporated water. With the new dry content (DC = 1) a new boiling point is calculated from to equation (12) and compared with the new temperature T_{new}. If the new temperature is higher than the boiling point, the assumption of complete evaporation is correct and no further calculation in this step is needed. In case it is lower, the assumption is wrong and further calculations must be performed to obtain the amount of evaporated water, m_{evap}, and the resulting temperature. This is done with the function *fzero* implemented in MATLAB that in this case minimizes the difference between the obtained temperature and the boiling point temperature by varying the amount of water that is evaporated. As initial value for the amount of water evaporated - representing a starting guess for the minimization - the whole energy accumulation in the section is used for evaporation. With the calculated amount it is possible to determine the changes in the water and gas content in the actual section.

The new gas accumulation is the sum of the preliminary value and the amount of water evaporated

$$m_{G,acc,new} = m_{G,acc} + m_{evap} \quad (16)$$

The solid content is not influenced by the evaporation.

As mentioned before, the program only allows either evaporation or pyrolysis to occur in one section. The check for pyrolysis is, therefore, only performed in case that no evaporation took place. For pyrolysis to occur, the temperature should be higher than the onset temperature and the amount of solids left, compared to the initial amount in the actual section, is taken into account. It is assumed that 40 w-% of the solids can be pyrolysed. A collection of experimental data for four different black liquors [4] indicates that the amount of dry solids pyrolysed can reach up to 40 w-% and is rather a function of the temperature environment than of the heating rate. Below 800 °C the dry mass pyrolysed is temperature independent and reaches little more than 30 % of the initial solid mass. The value of 40 w-% is therefore an over-estimation and will have to be checked with the experimental results. The pyrolysis reaction is expressed as a simple rate equation for two competing reactions giving r_{pyro}. This kinetically-limited model has also been used by Verril et al. [18] for modelling the devolatilization phenomenon during black liquor combustion.

$$r_{pyro} = \left[A_1 \cdot \exp\left(-\frac{E_1}{R \cdot T} \right) + A_2 \cdot \exp\left(-\frac{E_2}{R \cdot T} \right) \right] \quad (17)$$

where A_1 and A_2 are rate coefficients in [s^{-1}] and E_1 and E_2 the activation energies in [J/mol]. Since the rate parameters for black liquor are not known, the values for coal are used as done by Verril et al. [18] The mass of gases released is then calculated as

$$m_{pyro} = \frac{m_S \cdot r_{pyro}}{tstep} \quad (18)$$

Again, the equation has to be divided by the time step to account only for the time interval the calculations are made for. The amount of each species released is defined from the experiments by its fraction of the total released amount. The

accumulated energy in the section under consideration is reduced by the necessary energy for the pyrolysis process

$$q_{acc,new} = q_{acc} - m_{pyro} \cdot \Delta H_{pyro} \quad (19)$$

and the preliminary value for the gas mass accumulation is increased by the amount of gases pyrolysed

$$m_{G,acc,new} = m_{G,acc} + m_{pyro} \quad (20)$$

Finally, the amount of solids and gases is reduced respectively increased by the mass pyrolysed whereas the water content is not changed by the pyrolysis calculations.

After the calculations for evaporation and pyrolysis are finished the change in gas mass due to the flow between the sections is determined and the energy left is used for heating up the section.

$$m_{G,new} = m_{G,old} + m_{G,acc,new} \quad (21)$$

$$T_{new} = T_{old} + \Delta T \quad (22)$$

with $$\Delta T = \frac{q_{acc,new}}{m_S \cdot \left(C_{p,S} + C_{p,E}\right) + m_W \cdot \left(C_{p,W} + C_{p,E}\right) + m_G \cdot C_{p,G}} \quad (23)$$

Swelling

After the pyrolysis calculations, the swelling of the droplet is calculated. If the mass of gases in a certain section is increasing, swelling might occur. The incremental change in radius and volume for each section is calculated with a separate function giving the radius increase for the bubbles inside the section depending on the pressure differences.

$$dr = \frac{\frac{r_{bub} \cdot \Delta P}{4 \cdot \mu_{BL}} - \frac{\sigma_{surf}}{2 \cdot \mu_{BL}}}{tstep} \quad (24)$$

r_{bub} is the actual bubble radius at that time in [m], ΔP the pressure difference in [Pa] between the actual section and the next one in radial direction (the difference between the section and the surroundings for the outmost section),

σ_{surf} is the surface tension of black liquor [N·m] and μ_{BL} its dynamic viscosity [Pa·s]. The numerator in equation (24) gives a time dependent change and has therefore to be divided by the time step. The new bubble radius is thus the actual one plus the change.

$$r_{bub,new} = r_{bub} + dr \tag{25}$$

It is then possible to calculate the total volume increase of the section with the number of bubbles.

$$V_{inc} = n_{bub} \cdot \frac{4 \cdot \pi}{3} \cdot \left(r_{bub,new}^3 - r_{bub}^3 \right) \tag{26}$$

The increase of the section radius then results to

$$\Delta r_{section} = \left(\frac{3}{4 \cdot \pi} \left[\frac{4 \cdot \pi}{3} \cdot r_i^3 + V_{inc} \right] \right)^{1/3} - r_i \tag{27}$$

For the outmost section the intersectional radius r_i has to be replaced by the outer radius r.

With the radius change it is possible to get the new volume of the actual cell, and the radii and intersection radii of all the other cells are recalculated. For the calculation of the outermost cell, that is performed last each iteration, it simply results in

$$r_{new} = r + \Delta r_{section} \tag{28}$$

This then gives a new volume, porosity and pressure for each section. As soon as the pressure in all section doesn't change more than the predefined value (0.2 percent for instance) in every section compared to the guessed value, the calculations for one time step are finished.

Modelling of the heat transfer in the droplet

The heat transfer in the droplet and from the gas atmosphere to the droplet is essentially determining the gas release rate and the swelling behaviour during drying and pyrolysis. A low thermal conductivity inside the particle will lead to steep temperature gradients and, as a result, the droplet might still be drying in its centre while it already is pyrolysed in the outer section. Having a high thermal conductivity, the temperature gradients will be levelled out and the different phenomena will occur sequentially in the whole droplet. There have been several attempts to model the thermal conductivity inside a black liquor droplet. Frederick [13] approximated the intra-particle heat transfer by a simple thermal resistance model. Saastamoinen and Richard [21] used a correlation for the internal conductivity based on the assumptions that the material structure can be represented by cubical pores spaced at equal distances. Liquid water was assumed to be equally distributed at the pore walls. In analogy to electrical resistance nets, an effective conductivity could be obtained based on the heat conductivity of the different media, the porosity and the pore dimension. This correlation – including thermal radiation - was further developed and modified for black liquor by Järvinen et al. [22] and the following equation is proposed:

$$k_{eff} = k_{BL} \cdot \left(1-\phi^{2/3}\right) + \frac{\phi^{2/3}}{\frac{1-\phi^{1/3}}{k_{BL}} + \frac{\phi^{1/3}}{k_G}} + \frac{16 \cdot \sigma \cdot T^3}{3 \cdot a_R} \cdot \phi \qquad (29)$$

In equation (29), k_{BL} is the thermal conductivity of black liquor [W/(m·K)], k_G the one of the gases [W/(m·K)], ϕ the porosity of the droplet [-], σ the Stefan-Boltzmann constant [W/(m^{2}K^4)], T the temperature [K] and a_R the Rosseland adsorption coefficient [m^{-1}] that according to Järvinen et al. led to the best fit for a value of 850 m^{-1}.

This equation was used in the program replacing a constant assumed effective thermal conductivity. For the thermal conductivity of black liquor there has been an empirical equation established by Adams et al. [4] that is valid in the range of

0-82 % dry content and a temperature range of 20-100 °C. This range is not covering the changes to black liquor during drying, devolatilization and pyrolysis but according to the source it should be valid even for higher temperature ranges. The equation is:

$$k_{BL} = 1.44 \cdot 10^{-3} \cdot T - 0.335 \cdot DC + 0.58 \qquad [W/(m \cdot K)] \quad (30)$$

where T is the temperature in °C and DC the dry content.

Experimental part

Black liquor properties

The black liquor used for the experiments is black liquor originating from SÖDRA Cell Värö pulp mill. Its elementary composition is given in table 2. It is a typical composition of kraft black liquor and can therefore be used as basis for the modelling work. Kraft black liquor has, compared to other biomass, a high sodium content resulting from the cooking process.

Table 2: Elemental composition of the black liquor used for the experiments

Element	% of dry mass
Carbon, C	36,3
Hydrogen, H	3,1
Nitrogen, N	0,07
Sulphur, S	2,8
Chlorine, Cl	0,32
Sodium, Na	19,7
Potassium, Ka	2,44

The original dry content of the black liquor was given in the original analysis as 66 w-%. It was determined again by drying the black liquor in 130 °C and it was found that it had decreased to about 64 w-%. One reason for the difference might be the fact that black liquor is a hygroscopic material and the sample had been stored for some time. Another might be that during the drying process at 130 °C volatiles already have been released. The deviation is acceptably small and as the procedure of determining the dry content is not exactly known for the original measurement the value of 64 w-% has been used for the calculations.

Table 3: Dry content of the black liquor used for the experiments

Mass of sample [g]	Determined dry content [w-%]
1,574	64,24
1,585	64,16
1,738	64,13

Experimental setup

Experiments were performed to give useful data for improving the model and in particular the reaction kinetics. Therefore, a single droplet was exposed to a constant reactor temperature in a furnace tube and the released gases were analysed. The gas atmosphere during all experiments was nitrogen, as it was the goal to do pyrolysis with absence of any oxidizing media. The gas stream entered through a preheating section and then passed the droplet upwards in a vertical furnace tube. Three heating elements are installed along the tube to keep a constant gas temperature. The gases then passed through a cooling section and through a series of online gas analysers to monitor the four species CO_2, CO, CH_4 and SO_2. The droplet of black liquor was exposed to the gas stream on a thin thermocouple wire that is formed as a spiral to keep the droplet in a stable position. With this thermocouple, it was possible to monitor the droplets internal temperature during the experiment. Ideally, it would be the temperature at the centre of the droplet but this was seldom the case, as the droplet started melting and therefore moved from the end of the thermocouple, where the temperature was measured. But, at least, the measurement gives information about the temperature inside the droplet even though the exact point could not be defined. The mass of the droplet was measured by placing the thermocouple on a scale on top of the furnace tube. The scale was placed into a sealed box in order to avoid air intake into the reactor tube. The flow of nitrogen through the box, as well as through the reactor, was adjusted by online-controlled valves that were set to fixed values for all experiments. In order to examine the swelling behaviour of the droplet during the different processes occurring, it was possible to record the droplet through a window that is located at the height of the furnace tube where the droplet is pyrolysed. A schematic setup of the experimental equipment is given in figure 8.

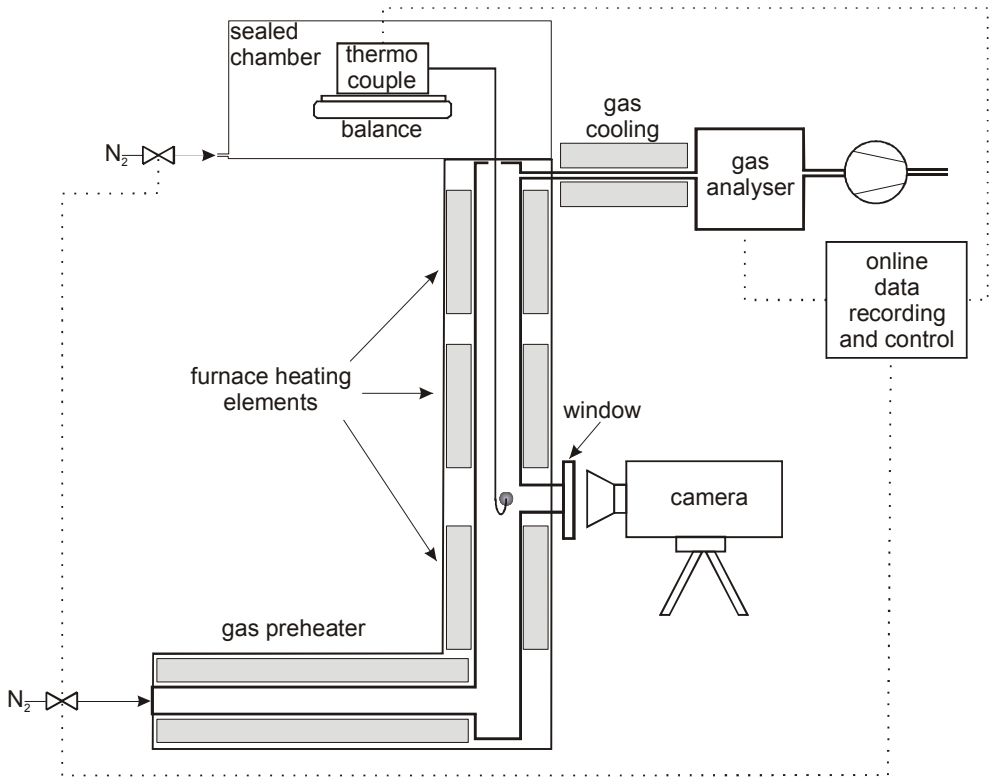

Figure 8: Schematic setup of the experimental equipment

The temperature range for the experiments was 275 °C to 400 °C. To make sure that no pyrolysis reactions occur at lower temperatures three runs were done at 200 °C.

Experimental procedure

The experiments were set up in the following way. First, the reactor heating was set to the desired temperature and the gas flow was set to a fixed value of 15 l/min through the furnace tube and 3 l/min through the box containing the balance. During the heating period the gaseous medium was air. The balance was set to zero with the thermocouple on it to be able to approximately measure the droplets weight during the experiment. When the reactor temperature was stable at its set value, a small droplet of about 3-4 mm in diameter was placed on the thermocouple and its weight determined by difference measurements. The gas flow was changed from air to nitrogen and as soon as the gas analyzers had

reached a constant level – the baseline – the experiments could be started. All of the first runs were also recorded on video tape, as this data will be used for improvements in the swelling modelling. In the end though, when repeating experiments the video camera was not used any more. The experimental procedure was to place the thermocouple on the balance and adjusting it to make sure that the wire, going into the furnace tube, does not touch anything. Otherwise the balance results were useless. The gas release was then measured and could be checked on-line on a screen. The experiments were run until all four gas measurements had reached the baseline again. This took, depending on the temperature, up to 10 min at maximum. Table 4 gives an overview of the experiments that were performed.

Table 4: Experiments performed

Date	Reactor Temperature [°C]	Runs performed	Used for evaluation
2004-10-28	275	10 (275 A-J)	0
2004-11-02	325	5 (325 A-E)	0
2004-11-03	325	5 (325 F-J)	2 (F/H)
2004-11-03	350	5 (350 A-E)	3 (C/D/E)
2004-11-10	350	5 (350 F-J)	2 (F/G)
2004-11-10	375	10 (375 A-J)	6 (C/E/F/H/I/J)
2004-11-16	275	10 (275 K-O)	6 (L/P/Q/R/S/T)
2004-12-01	200	5 (200 A-E)	0
2004-12-01	325	5 (325 K-O)	3 (K/L/N)
2004-12-01	350	5 (350 K-O)	0
2004-12-17	300	5 (300 A-E)	5 (A/B/C/D/E)
2004-12-17	375	5 (375 K-O)	5 (K/L/M/N/O)

The choice of experiments used for evaluation was based on the quality of the gas measurements on the one hand and on the usefulness of the balance measurements on the other hand where, of course, the gas measurements were more important as it is the goal to improve the reaction kinetics which is directly related to that property. The measurements at 200 °C were only to control that no measurable release of gases occurred at these low temperatures and were therefore not taken into account in the further evaluation.

In addition to the experiments listed above, there was data available from experiments performed by Joko Wintoko, a PhD student at the department, at temperatures of 300 and 400 °C. The data from the experiments at 400 °C was used in order to expand the temperature range.
In order to be able to reconstruct the actual gas release at the droplet during the experiments with the method of deconvolution, it was necessary to do trace experiments at each temperature to determine the dead time of each gas species analyzer and the residence time distribution (RTD) of each gas. This was done by replacing the glass window, normally used for the video camera, by a lid with a small hole. Through this small hole, a gas mixture of CO, CO_2, CH_4 and SO_2 was injected via a small pipe in order to release the gas approximately at the same position where the droplet is situated during a normal experiment. The residence time and the response of the gas analyzers were recorded to be used later on for the deconvolution process.

Data treatment and results

The raw experimental data had to be treated to make conclusions regarding the mass balances and to be able to compare it to the simulation results. In a first step, the starting point of the experiment was determined with the help of the temperature measurements that gave a peak when the thermocouple was inserted in the tube furnace. Then the base-line for each gas species was subtracted and the resolution of the measurement taken into account. The raw data had to be changed as the analyzers had a higher resolution in the low concentration regime, below 100 or 200 ppm depending on the analyzer. Finally, the online measurements of the balance were adjusted to the initial weight of the droplet. The online balance measurements can be seen as relative measurements as the influence of the drag due to the gas flow around the droplet cannot be exactly determined. So the initial weight was determined at a very early point in the measurement and the whole curve shifted by the difference between that value and the absolute weight value of the droplet that had been

determined before the experiment. Examples of such curves are shown in figures 9 and 10.

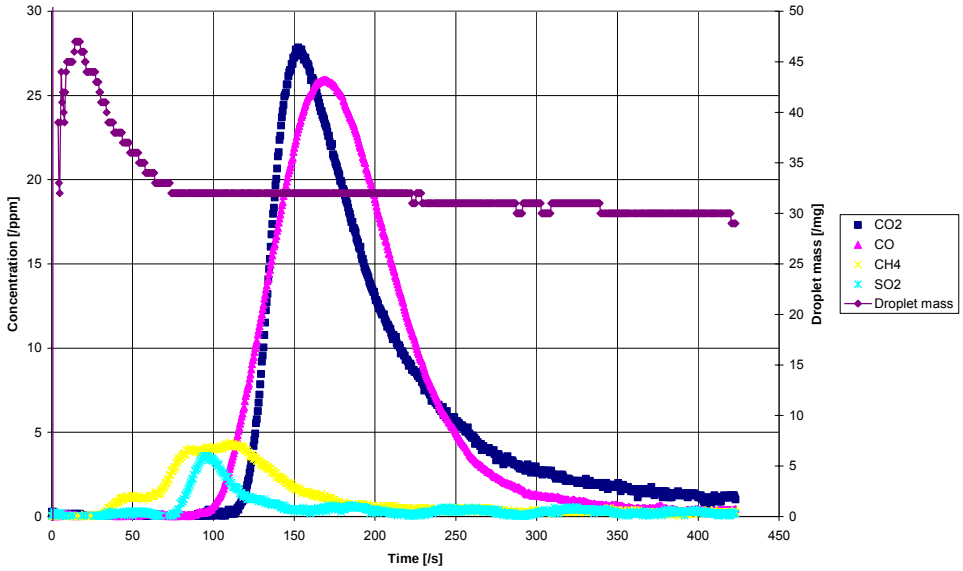

Figure 9: Gas release and droplet mass for experiment 375 K

In figure 9, the measured gas release in [ppm] for all four gas species CO, CO_2, CH_4 and SO_2 is represented, as well as the balance measurements. It can be seen that the droplet mass decreases fast in the beginning, due to evaporation and gas release, but reaches a steady level at the end of the experiments. The balance measurements fluctuate severe in the beginning making it hard to determine the initial mass of the droplet during the experiment. The gas analyzers respond at a different time for each gas species. This is mainly due to the individual dead-time of each analyzer and this effect will be accounted for with the method of deconvolution. The temperature profile shown in figure 10 shows a plateau at a time of about 25 sec. This is the time when the water is evaporating inside the droplet and the temperature rise therefore is decelerated. The average temperature increase for the droplet can vary between 3 and 7 °C/s in the temperature range of 300 to 400 °C.

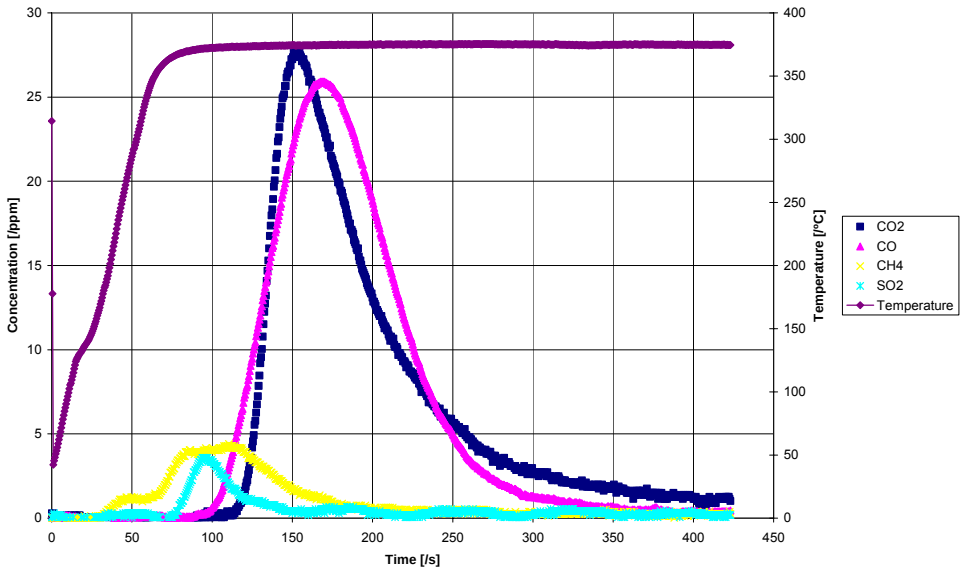

Figure 10: Gas release and temperature profile for experiment 375 K

Mass balance

The general mass balance for the pyrolysis experiments performed can be decribed as in figure 11.

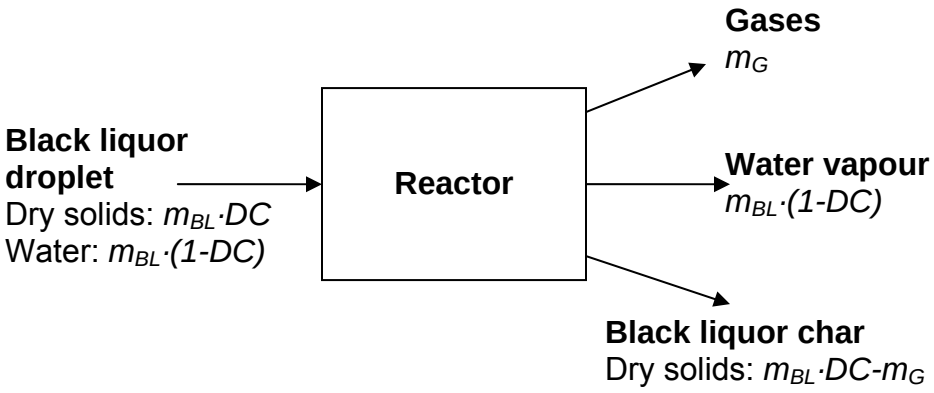

Figure 11: General mass balance

This must of course be seen as a simplified balance, for example water vapour may contribute to reactions with the black liquor solids resulting in additional gas release, but for basic investigations regarding low temperature pyrolysis it is sufficient. Another assumption, in this method, is that the black liquor char is

completely dried. This should be the case, as the droplets are small enough to get completely dried in an environment of about 300 to 400 °C. To get an idea of the amount of gases released in comparison to the initial dry mass of the droplet, respectively in relation to the dry mass loss, and of the ratio of different gases released at different temperatures the data on these quantities were investigated more detailed. Figure 12 gives the dry mass loss for several experiments and an average value at each temperature. Since the initial mass varied for the different experiments, the mass loss is given as percentage of the initial dry mass.

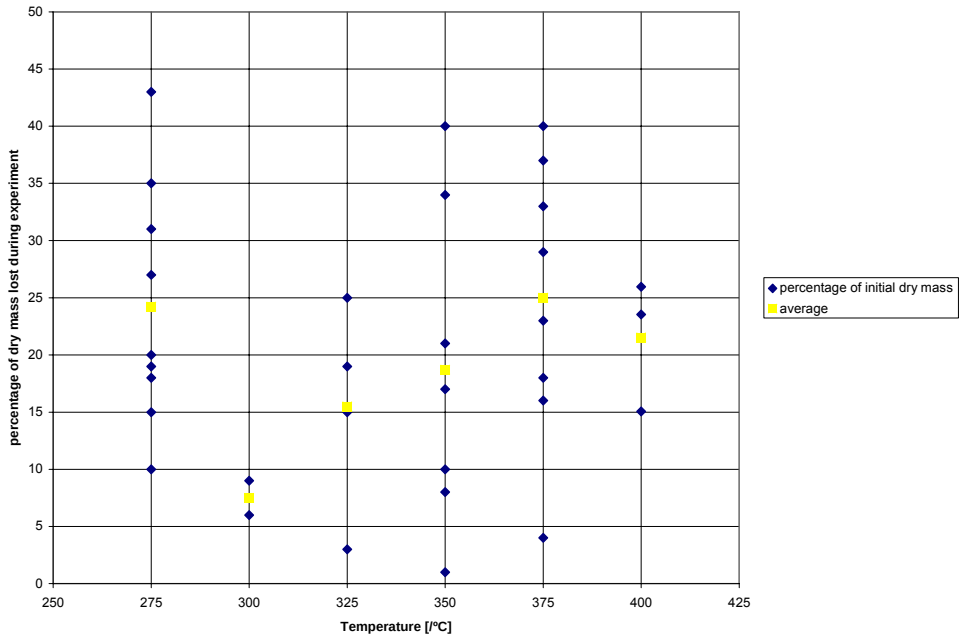

Figure 12: Dry mass loss during experiments

The data shows a wide spreading for each temperature. This is mainly due to the difficulties of properly shifting the measured balance data to the right value. The initial mass of the droplet can be determined correctly but the final weight is taken from the measured balance curve. This curve, as already mentioned, had been shifted to the initial weight at a very early time in the experiment. But, as can be seen in figure 9, the weight measurements are fluctuating much in the beginning, making it difficult to decide the initial weight in the experiment. This has, of course, a direct influence on the value of the final weight as the whole curve is shifted and therefore is influencing the dry mass loss. The values vary between 1

and 43 percent as a maximum. When looking at the average values, a tendency of increasing mass loss with increasing temperature from 300 to 400 °C can be seen. This seems reasonable as an increase in pyrolysis gas production can be assumed with increasing temperature resulting in a higher dry mass loss. The high average mass loss at 275 °C cannot be explained. As the data is fluctuating a lot and the trend starting from 300 °C render the value of 275 °C very unlikely to represent the reality, this temperature range has been left out for the further calculations and evaluations.

Table 5: Weight-fraction of the measured gas species (accumulated amount)

Fraction of gases species released (mass-based)	CO_2 [/%]	CO [/%]	CH_4 [/%]	SO_2 [/%]	sum [/%]	% of initial dry solids
300 °C	45,96	47,90	3,21	2,94	100	3,55
325 °C	43,28	50,87	3,16	2,69	100	2,11
350 °C	63,22	32,36	1,90	2,52	100	1,41
375 °C(1)	50,94	41,09	2,30	5,68	100	1,18
375 °C(2)	55,19	38,34	3,47	3,00	100	7,37
400 °C	63,30	30,91	2,43	3,36	100	7,47

Further on, the ratio of the accumulated amount for the different released gases was examined. Table 5 gives the fraction of the measured gas species at the different temperatures. The two gas species CO_2 and CO make up over 90 w-% of the measured released gases for all temperatures. In the investigated temperature range, the fraction of CO_2 has an increasing and the CO fraction a decreasing tendency. The fraction of both CH_4 and SO_2 is around 3 w-% for nearly all temperatures. A plot of the accumulated released gases and the sum of the four gas species can be seen in figure 13. The values are all averages of the evaluated experiments (see table 4). At the temperature of 375 °C there are two data series represented. This is due to the fact that the two series of experiments conducted showed very different results considering the amount of gases released. It can be seen that CO_2 and CO are the main species being released. A tendency for increased gas production is hard to see though. CO_2 gas production is increasing from 375 to 400 °C, whereas the CO release is

decreasing and the overall gas production is about the same for both temperatures. This might be due to different reactions occurring, having different mechanisms. As black liquor is a product based on wood, it contains a number of different organic species that take part in several reactions. The data might also give reasons to question the reliability of the measured gas release data.

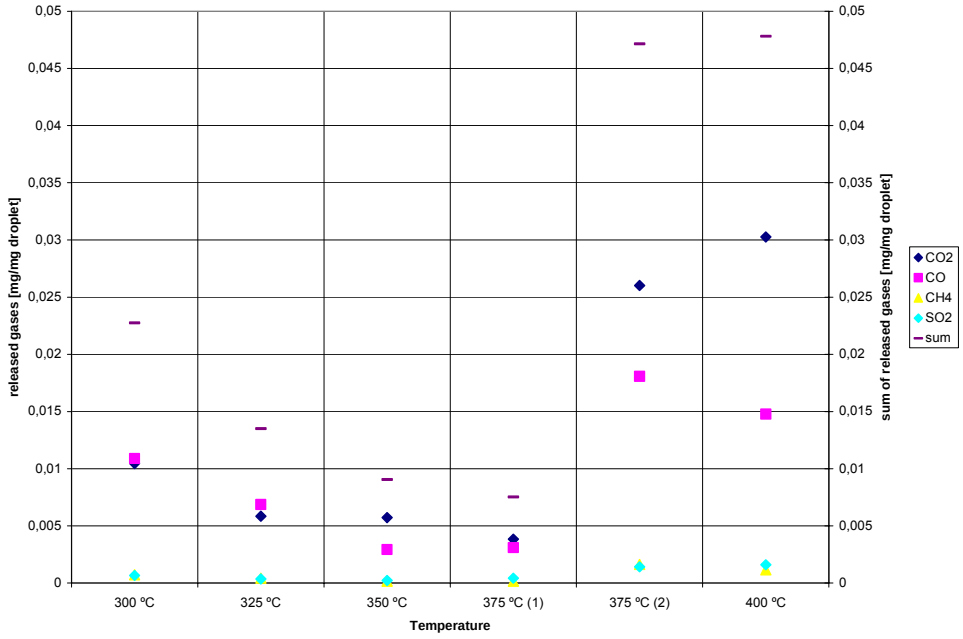

Figure 13: Release of different gas species at temperatures from 300-400 °C

Figure 13 shows a decrease of released measured gases in the range of 300 to 375 °C whereas the dry mass loss increases in the range as can be seen in figure 12. This clearly shows that there must be a considerable amount of other gases released that are not measured.

It is an interesting point to know what fraction the four gases measured during the experiments represent compared to all gases released. Therefore, the released amount of gases was set into relation to the dry mass loss that is assumed to be completely converted to gases. As the dry mass loss measurements are quite uncertain, figure 14 also represents the ratio of released gases in comparison to assumed dry mass losses of 5, 10, 20, 30 and 40 w-%. Looking at the experimental dry mass losses it can be stated that the measured gases make up 5 to 50 % of the dry mass loss but without showing any trend correlated to

temperature. For the assumed values the measured gases of course make up a higher fraction for lower dry mass losses. It can be seen that the assumption of only 5% of dry solids being converted seems to be wrong, as the measured gases are more than this amount for 375 and 400 °C (the ratio is bigger than 1) in that case. The experimental data indicates dry mass loss in the regime of 20 w-% as can also be seen from figure 12.

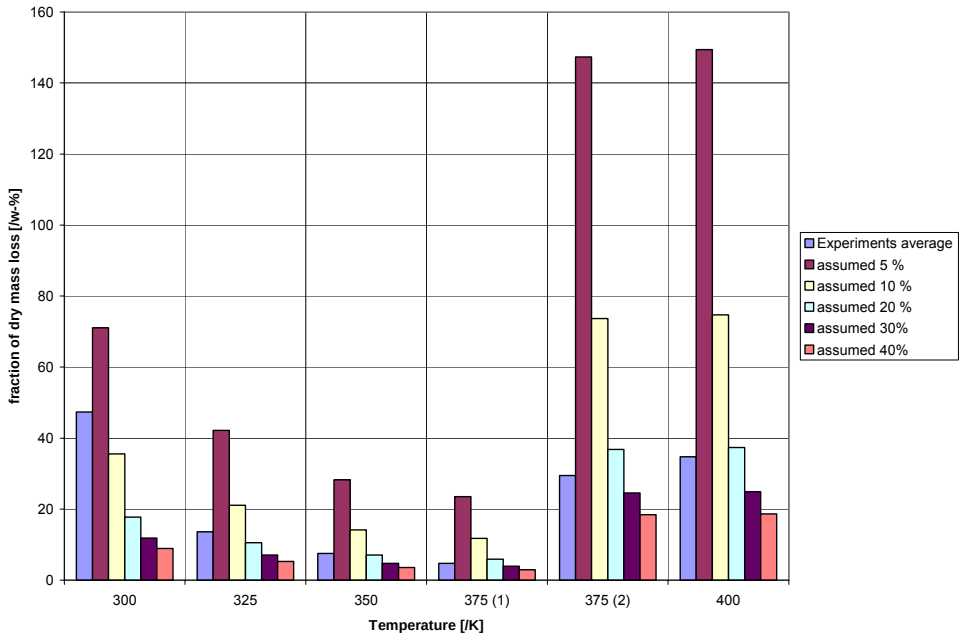

Figure 14: Ratio of measured released gases to assumed dry mass loss

For the experiments at 400 °C further investigations could be done as an elemental analysis of the black liquor char resulting from the pyrolysis experiments was done. The dry content of the char is assumed to be 1 and its elemental composition is given in table 6.

Table 6: Elemental analysis of black liquor char pyrolysed at 400 °C

Element	Weight-%
Carbon, C	33,2
Hydrogen, H	2,3
Nitrogen, N	0,06
Sulphur, S	2,5
Chlorine, Cl	0,76
Sodium, Na	27,2
Potassium, Ka	3,34

Based on the sodium content of both the original as well as the pyrolysed sample a dry mass loss can be calculated based on the assumption that no sodium is lost during pyrolysis. The calculated dry mass loss in this case results to 27.6 %. Based on the same assumption for potassium 26.9 % of dry mass loss are obtained. With the measured gas release it is possible to calculate the mass of each element and to compare it to the elemental mass loss, again using the experimental average value and assumed mass loss percentages.

Table 7: Element release at 400 °C

Element	Amount [mg/mg droplet]
C	0,0155
O	0,0313
H	0,0003
S	0,0008
sum	0,0478

Table 8: Elemental ratio of released gases to dry mass loss

Percentage of measured released gases based on dry mass loss						
	21,52% w-loss (experimental average)	5% w-loss	10% w-loss	20% w-loss	30% w-loss	40% w-loss
C	23,58	50,74	37,62	24,80	18,49	14,74
H	3,51	4,97	4,41	3,61	3,05	2,64
S	14,96	29,50	22,80	15,67	11,94	9,64

When assuming the dry mass weight loss to 20% this means that only about a quarter of the elemental carbon that is lost is converted to the gases CO, CO_2 and CH_4. The other three quarters result in higher molecular gas molecules and tars. For hydrogen and sulphur these values are even lower. One sulphur-containing species that is expected to be produced, but is not analysed is for example H_2S. When assuming lower dry mass losses the ratio obviously increases. But the carbon ratio is 50 % at the maximum when assuming 5 % weight loss – what is a too low value as already stated. This shows that more than half of the carbon is definitely converted to other species.

Data preparation for kinetic parameter analysis

To improve the kinetic model for the gas release during pyrolysis it is necessary to convert the measured gas release data. A MATLAB routine converting it to the expected real time data of gas release at the droplet was applied on the raw data. A method of deconvolution was used that had been proved to be very useful for investigation of coal pyrolysis kinetics [23]. The method uses the trace analysis – assuming that the tracer has been injected instantaneously – to convert the measured data to the real release data. This is done by first zero-time-adjustment and normalization of both the tracer and measured data followed by a fourier transformation in combination with a filter algorithm to prevent nonsense results due to the adaptation. To check the reliability of the applied procedure, the deconvolved data is then convolved again with the help of the tracer data, and the fit with the originally measured curve can be checked. This is useful as deconvolution is quite a complicated process whereas the convolution is quite easy to do and reliable, therefore serving well as a measure to check the correctness of the results. Figure 15 shows the normalized and zero-time adjusted curves of the tracer and measured data. The deconvolved curve, with both the originally measured one, and the curve again convolved to check the correctness of the result, can be seen in figure 16. Both curves are for an experiment at 375 °C (375 K) and applied for the species CO.

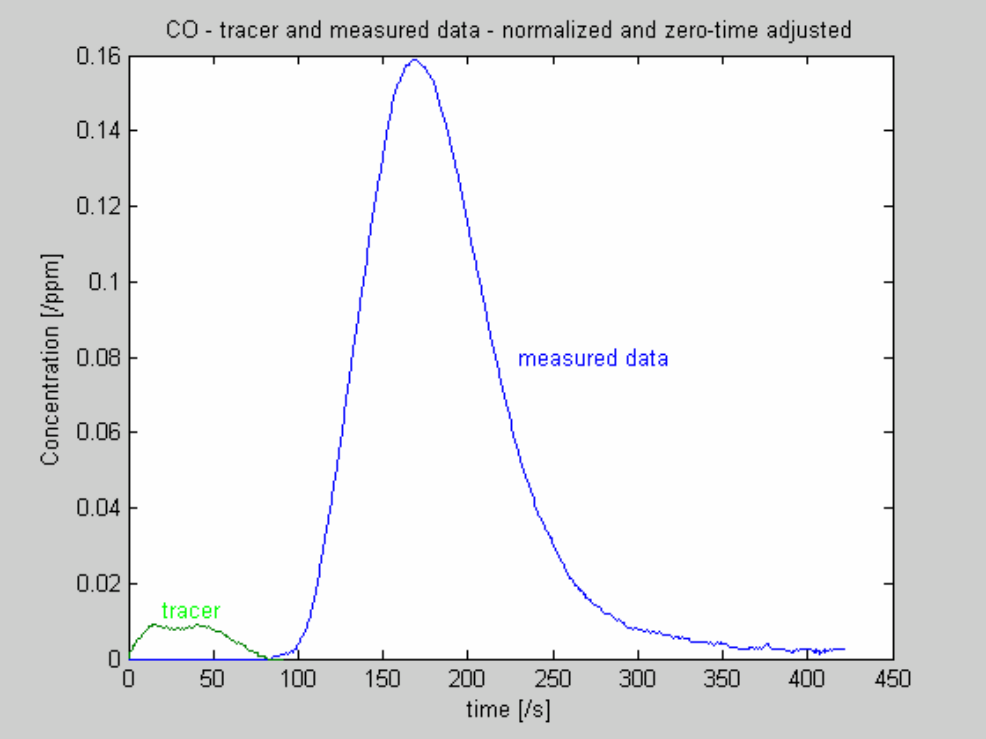

Figure 15: Zero-time adjusted and normalized tracer and measured data curves (Experiment 375 K – CO)

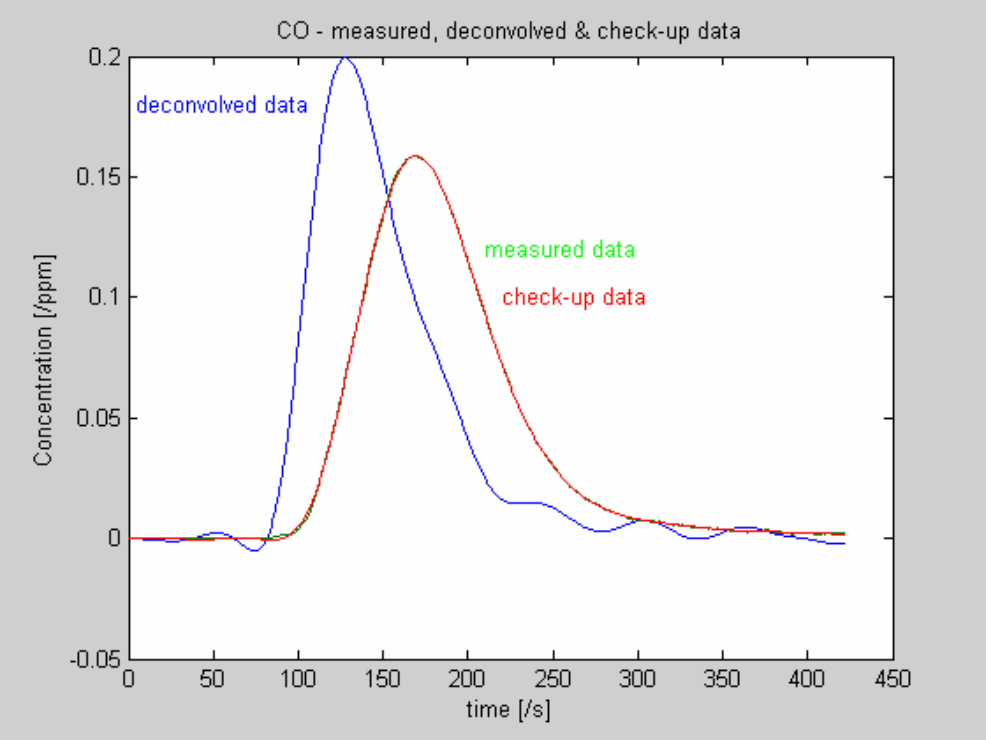

Figure 16: Deconvolved curve and originally measured as well as check-up curves (Experiment 375 K – CO)

As can be seen from the graph in figure 16, the fit between the originally measured curve and the check-up curve is good which implies that the method worked properly. It has, though, to be taken into account that all calculations are based on the residence time distribution of the tracer amount and it cannot be guaranteed that this data is completely correct. Another requirement for the theory of deconvolution to be applicable is that the detector response is related linearly to the species concentration. For species that are only released in very low concentrations, the fit was worse as the Butterworth filter algorithm used in the routine had difficulties handling the noises in the measured data that, in relation to the measured values, increased. This caused problems especially for CH_4 and SO_2 that were only produced in small amounts in the lower temperature regime.

In addition, it has to be taken into account that the analyzing equipment should be as close to the source of release as possible to reduce possible errors. The dead-time of the equipment used is quite long and, thus, giving reasons to handle the obtained data with care. This dead-time – being close to 40 seconds in some cases – still had to be taken into account for each individual species and temperature. The curves had to be shifted on the time axis to give the release directly at the droplet. This then resulted in a gas release as presented in figure 17. It can be seen that the gas release starts approximately at the same time for all species. The fact that the concentration is below 0 for some curves is due to numerical errors in the deconvolution process and does, of course, not reflect the reality. These negative concentrations have been zero-padded for the further evaluation of the data considering the adjustment of the kinetic parameters in the simulation program.

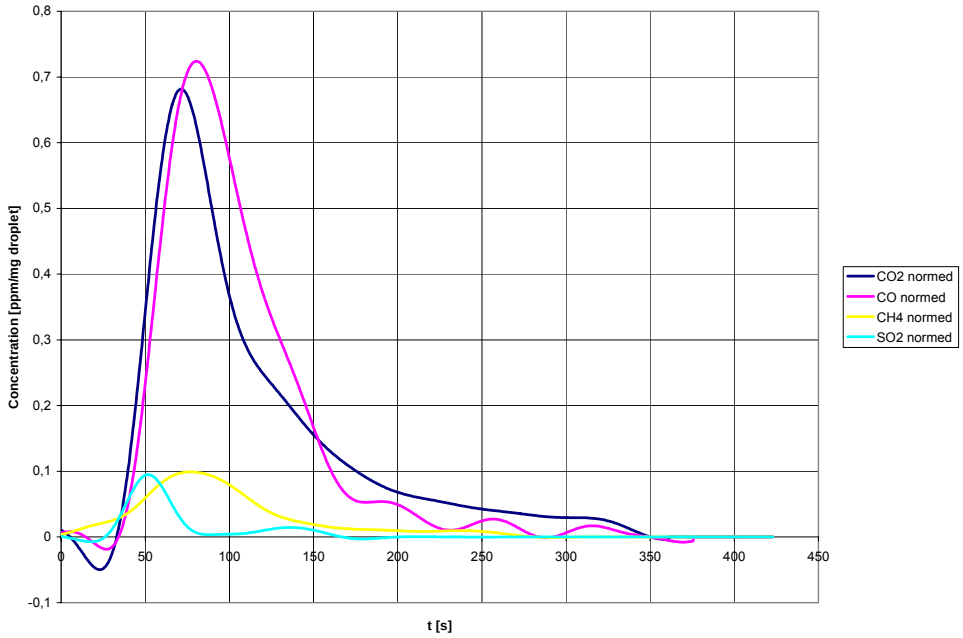

Figure 17: Deconvolved gas release directly at the droplet, Experiment 375 K

In order to have an average data to be used for comparison to the simulated gas release the release, was normalized by mass to equal the release of 1 mg of black liquor and an average of all experiments at each temperature was taken.

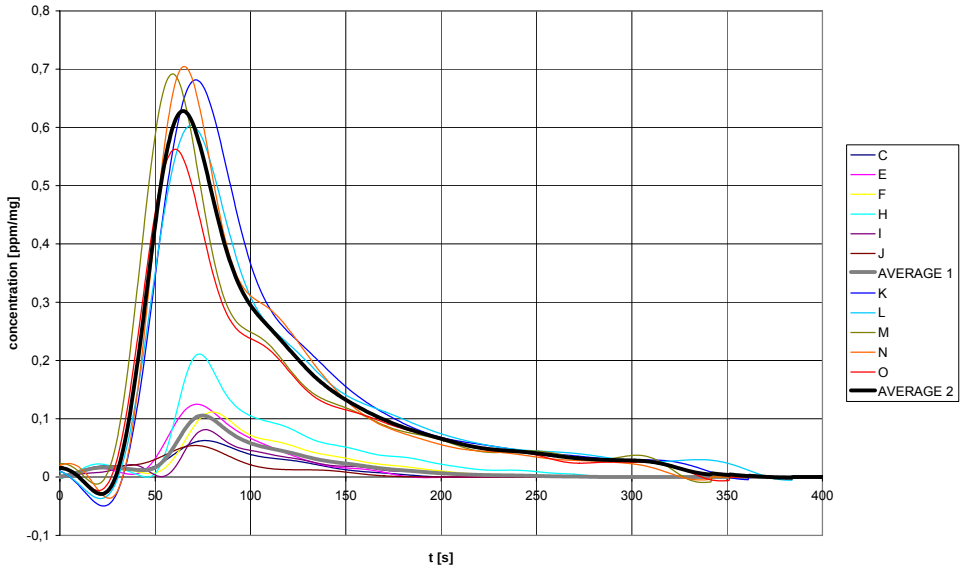

Figure 18: Normalized CO_2 release for all experiments at 375 °C

Again, there are two different averages, due to the very different results for two series of experiments at 375 °C. The deviation of the different experiments from the average is acceptably small for CO_2 and CO but for CH_4 and SO_2 the relative deviation increases as the absolute value for the deviation is about the same but the signal value is smaller. This fact has to be taken into account for all gas species when the temperature is decreased, due to lower release. One important point that can be stated is that the time when the gas release started was about the same in all experiments. As the temperature profile for all experiments is the same this indicates that there is a distinct temperature when the reactions start.

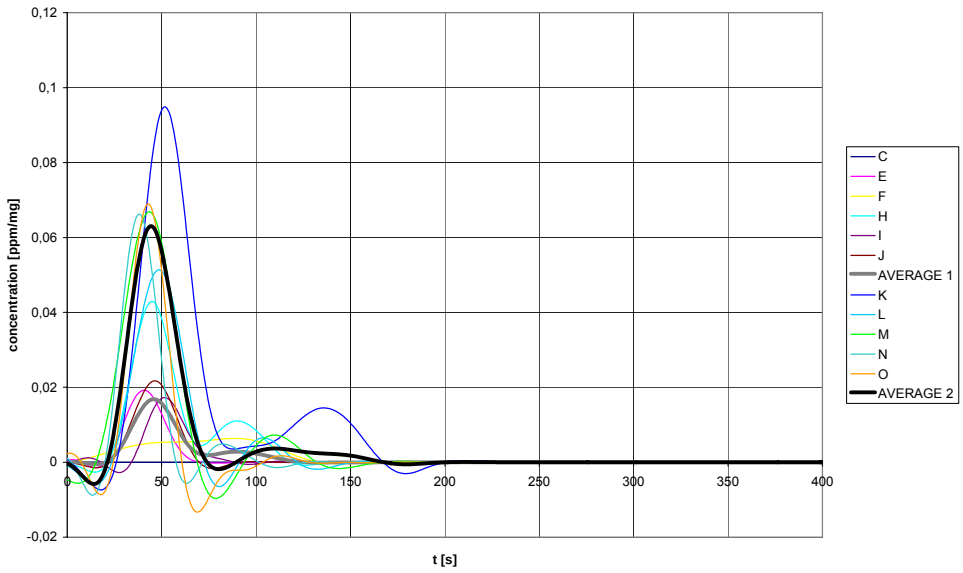

Figure 19: Normalized SO_2 release for all experiments at 375 °C

The normalization and averaging led to release data for all four species CO_2, CO, CH_4 and SO_2 at temperatures of 300, 325, 350, 375 and 400 °C. To be able to compare the data to the simulation the accumulated amount was calculated by integration. The mass of released gases per mg droplet is used as unit and the values are adjusted to the droplet mass used for the simulations later on.

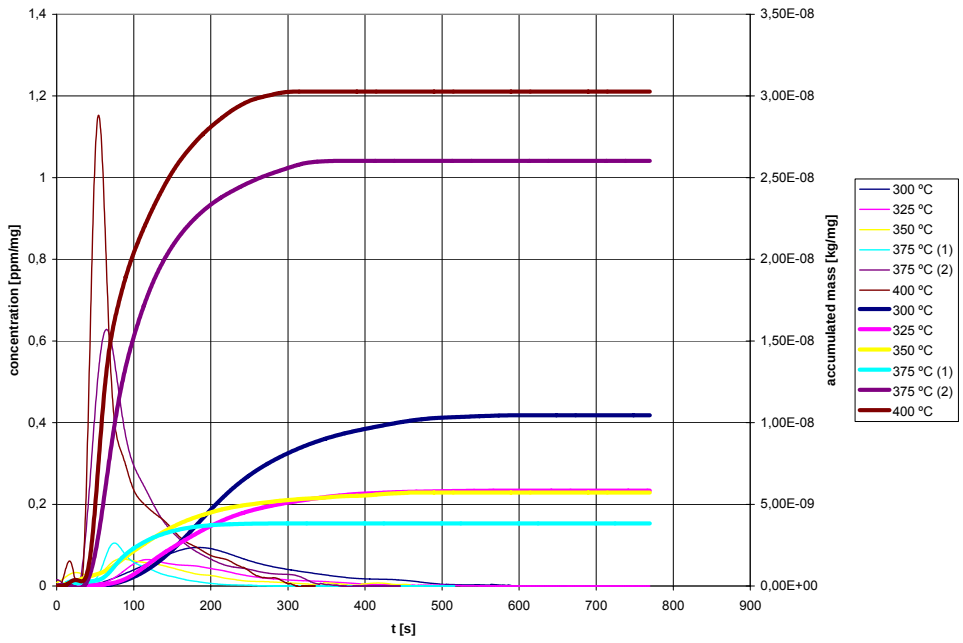

Figure 20: Normalized CO_2 release in the range of 300 to 400 °C

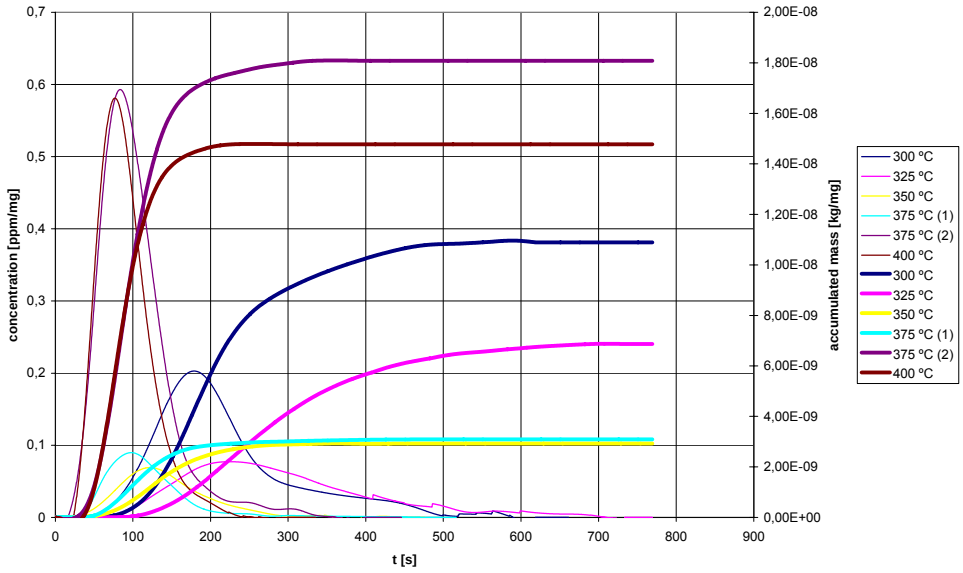

Figure 21: Normalized CO release in the range of 300 to 400 °C

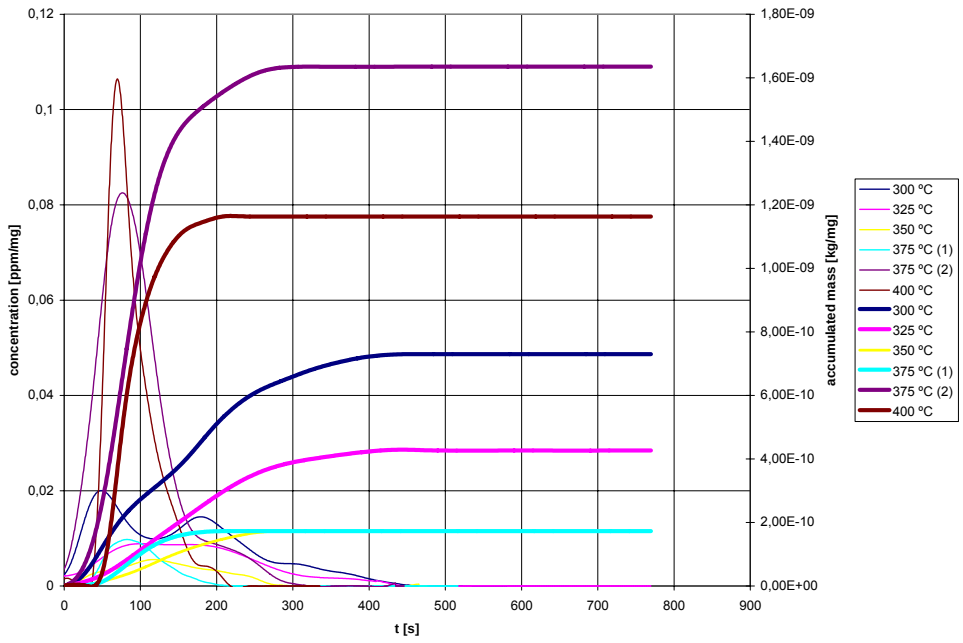

Figure 22: Normalized CH_4 release in the range of 300 to 400 °C

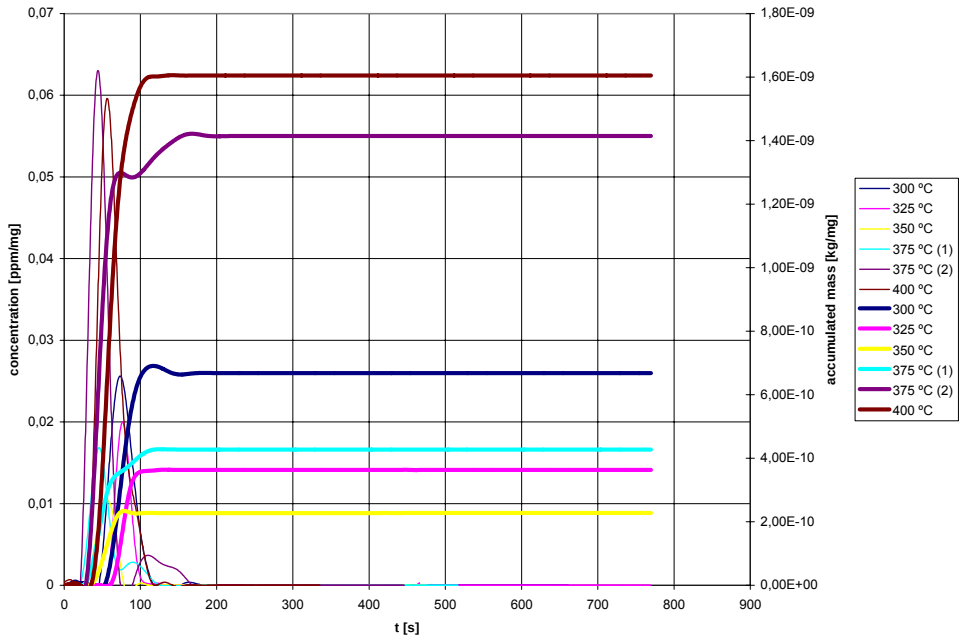

Figure 23: Normalized SO_2 release in the range of 300 to 400 °C

From the graphs it can be clearly seen that there is an increase in gas release with increasing temperature. The dominating gases are CO and CO_2 and minor release can be detected for CH_4 and SO_2. For lower temperatures - 350 °C and below – the release data has to be handled with care as the signal-to-noise-ratio

is decreasing and it becomes difficult to see clear trends. Looking at the two main species, CO and CO_2, the temperature dependence of the gas release seems to differ as the CO_2 release is increasing from 375 to 400 °C whereas the amount of CO released is decreased by that temperature rise. Also for CH_4, the amount released is getting smaller at 400 °C compared to 375 °C. The overall gas release doesn't change between these two temperatures as can be seen from figure 13, where the accumulated amount of gases released is plotted for the different temperatures. This gives reason for further investigations on the behaviour in higher temperature regimes.

Adjustment of kinetic parameters

The goal with adjusting the parameters is to get representations of the gas release from the simulations that fit well to the experimental data. Therefore, optimization routines were applied to modify the kinetic parameters – namely the collision frequency factors and activation energies – in order to get a better fit of the release curves. In order to carry out the optimization within in a reasonable period of time, it was necessary to write a new, simpler program for calculating the gas release. The original program took between two and three hours to finish the calculations for an experiment of 350 seconds. As several hundred calculations are necessary for the optimisation algorithm to search for improved values it is practically impossible to do the optimisation on the original program. Therefore, a simplified program was developed to optimize the parameters. This program used data from a calculation with the original program to compute the gas release. Based on the calculated temperature profile it checked only for pyrolysis reactions in each section and gave the accumulated gas release for each section as result. To get comparable values to the experimental data, only the values at each 0.5 seconds were picked from the temperature profile, which increased the speed of calculation even further. A simplification in this program, that has to be considered, is the fact that it adds up all produced gases whereas the original program only calculates the gases actually released from the droplet

which is closer to the real case in the experiment. This simplification though introduced an acceptably small error of 2.3 % for all species as can be seen in figure 24 showing the overall CO_2 and CO production and the release of the two species for the basic case at 375 °C.

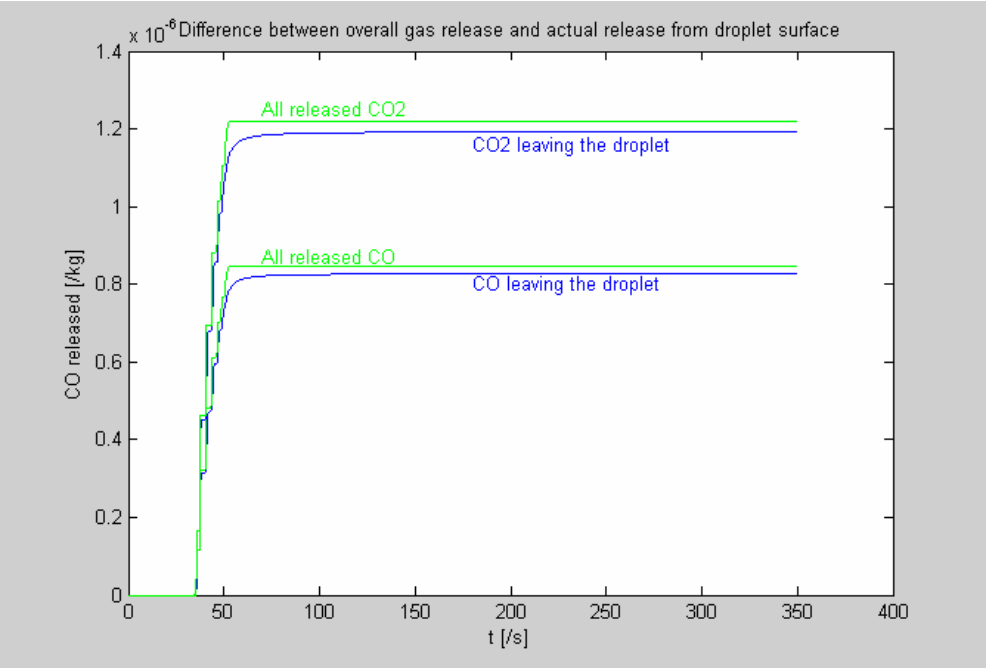

Figure 24: Difference between overall release and gases leaving the droplet for the simulation

This program was then used as a function for the optimization algorithm, returning the sum of squares of the difference between the measured and calculated amount of gases for each time. A droplet with a diameter of 4.2 mm was used, having a weight of 46.55 mg. This represents a good average of the experimental range.

Optimization algorithms

Several algorithms implemented in MATLAB such as *lsqnonlin*, *fmincon* and *fminsearch* were tested. The one that gave reasonable results for most of the cases that were tested in the beginning was the SIMPLEX algorithm developed by Nelder and Mead [24] and implemented in MATLAB as function *fminsearch*. It therefore was decided to use this algorithm for the optimisation. The SIMPLEX algorithm is more robust and doesn't use any information about Jacobian or Hessian matrices. This might result in longer iterations but is as well more stable. The other algorithms are numerically calculating derivatives to get a Jacobian matrix what may result in faster convergence but also implies more numerical problems. As acceptable results were obtained with the SIMPLEX algorithm it was considered sufficient to use this method.

Optimization results and discussion

The focus of the optimization is on the two temperatures of 375 and 400 °C as the experimental data is most reliable there. In a first step, the kinetic parameters are adjusted for 375 °C. The adjustment was done for the CO release with using the obtained ratio of gas release for 375 °C from the experiments (see table 5). The amount of gases released was limited by setting a maximum value for the dry solid mass that could be converted as this was the only feasible way to limit the production of gases. This value is less than 10 % for the measured gases in all experiments what is a lot less than the initially used value of 40 % in the simulation program. But it has to be considered that there are other gases produced as stated in the experimental part. Therefore the amount of solids that can be pyrolysed was kept at the initial 40 % to calculate reaction kinetics for all gases released but the amount of each gas species was limited to the corresponding experimental amount.

It showed that there are several sets of parameters giving good fit for the gas release. With different starting guesses for the four parameters A_1, E_1, A_2 and E_2 different final values were obtained. The starting guess for the first optimisation was the literature data that originally was used in the program. As a second try, the values were decreased to 50 % and finally very low values were used as starting guess. As the result for that last try gave no physically feasible solution – a negative collision factor A_2 was obtained – it was decided to try the option of representing the resulting reaction kinetics with only one reaction. Therefore, the reaction kinetics were calculated for a temperature range of 250 to 500 °C with the starting guesses for four parameters. From a linearized plot of $ln\ r_{pyro}$ over $1/T$ the two kinetic parameters for a single reaction then could be calculated and used as starting guess for the optimization with only two parameters. The results of the optimisation based on CO are shown in table 9.

Table 9: Optimization results at 375 °C based on the CO release

		Starting guess	1 (4 parameters)	2 (2 parameters)
A	A_1 [/s^{-1}]	$3.7 \cdot 10^5$	$3.46 \cdot 10^5$	18.55
	E_1 [/(J/mol)]	$7.36 \cdot 10^4$	$9.7 \cdot 10^4$	$4.45 \cdot 10^4$
	A_2 [/s^{-1}]	$1.46 \cdot 10^{13}$	$1.33 \cdot 10^{13}$	-
	E_2 [/(J/mol)]	$2.51 \cdot 10^5$	$2.6 \cdot 10^5$	-
	Residual sum of squares	$5.13 \cdot 10^{-11}$	$4.39 \cdot 10^{-13}$	$3.00 \cdot 10^{-13}$
B	A_1 [/s^{-1}]	$1.85 \cdot 10^5$	$8.86 \cdot 10^3$	$6.25 \cdot 10^4$
	E_1 [/(J/mol)]	$3.68 \cdot 10^4$	$7.75 \cdot 10^4$	$5.37 \cdot 10^4$
	A_2 [/s^{-1}]	$7.30 \cdot 10^{12}$	$1.7 \cdot 10^{12}$	-
	E_2 [/(J/mol)]	$1.26 \cdot 10^5$	$2.01 \cdot 10^5$	-
	Residual sum of squares	$7.73 \cdot 10^{-6}$	$3.86 \cdot 10^{-13}$	$6.02 \cdot 10^{-11}$
C	A_1 [/s^{-1}]	1	0.61	0.81
	E_1 [/(J/mol)]	100	$1.89 \cdot 10^2$	44.16
	A_2 [/s^{-1}]	1	-0.60	-
	E_2 [/(J/mol)]	100	$1.39 \cdot 10^2$	-
	Residual sum of squares	$1.13 \cdot 10^{-9}$	$2.85 \cdot 10^{-13}$	$4.52 \cdot 10^{-11}$

The fit has been improved by the optimization, decreasing the residual sum of squares by about two orders of magnitude. This also can be seen by plotting the simulated and experimental CO release curve for both the initial and a set of optimized parameters (A1).

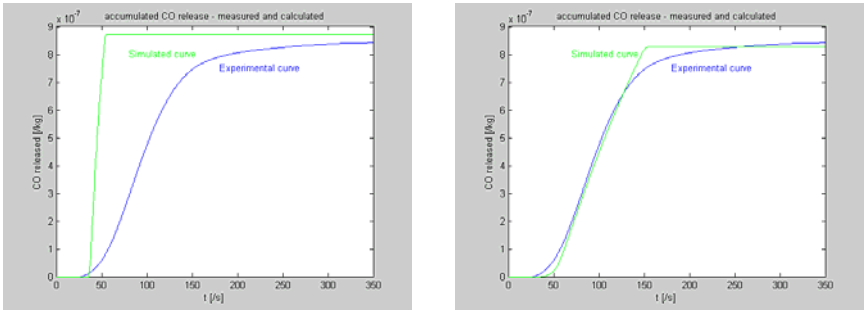

Figure 25: Initial and optimized CO release curve for 375 °C – simplified program

The optimized curves start increasing later than the experimental ones, due to the constraint that pyrolysis reactions only are allowed to occur above 300 °C. They have a steeper slope and in addition nearly the same shape for all parameter sets. The three sets of parameters for two reactions have a low residual and result in a good fit. For a single reaction, only the first set of parameters gives a good fit. To further investigate the values for the reaction kinetics, the resulting r_{pyro} for the temperature range of 250-450 °C has been plotted in figure 26. The values for r_{pyro} for the two sets C1 and C2 with very low starting guesses are nearly temperature independent. Although the optimized set C1 results in the lowest residual, both are unlikely to represent the real case. The set B2 gives even higher reaction kinetics than the initial set of parameters explaining the higher residual for this set. The best fit was obtained for the three sets A1, A2 and B1.

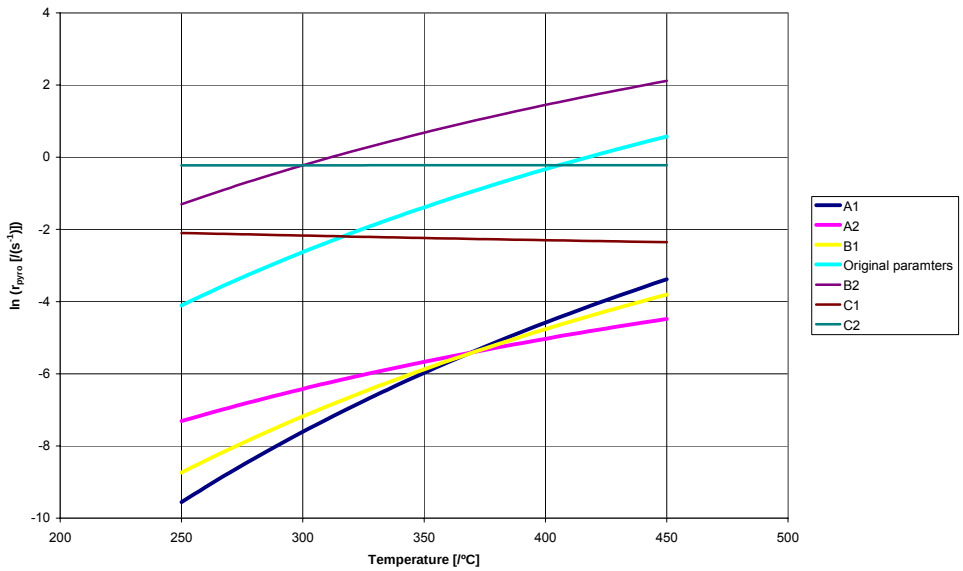

Figure 26: Resulting r_{pyro} for different kinetic parameters

In a next step, the change in results for the optimized parameters depending on the chosen gas species for optimization was examined.

Optimized parameters were found for starting points of the sets A1, A2 and B1, fitting the calculated and experimental gas release curves with the *fminsearch* algorithm.

Table 10: Kinetic parameter sets for optimization based on different gas species release data at 375 °C

		CO	CO_2	CH_4	SO_2
A1	A_1 [/s^{-1}]	$3.46 \cdot 10^5$	$3.62 \cdot 10^5$	$3.58 \cdot 10^5$	$3.57 \cdot 10^5$
	E_1 [/(J/mol)]	$9.7 \cdot 10^4$	$9.77 \cdot 10^4$	$9.68 \cdot 10^4$	$7.93 \cdot 10^4$
	A_2 [/s^{-1}]	$1.33 \cdot 10^{13}$	$1.28 \cdot 10^{13}$	$1.32 \cdot 10^{13}$	$1.45 \cdot 10^{13}$
	E_2 [/(J/mol)]	$2.6 \cdot 10^5$	$2.83 \cdot 10^5$	$2.90 \cdot 10^5$	$2.72 \cdot 10^5$
A2	A_1 [/s^{-1}]	18.55	12.37	11.44	115.08
	E_1 [/(J/mol)]	$4.45 \cdot 10^4$	$4.27 \cdot 10^4$	$4.14 \cdot 10^4$	$3.84 \cdot 10^4$
B1	A_1 [/s^{-1}]	$8.86 \cdot 10^3$	$1.23 \cdot 10^4$	$1.11 \cdot 10^4$	$2.77 \cdot 10^4$
	E_1 [/(J/mol)]	$7.75 \cdot 10^4$	$7.98 \cdot 10^4$	$7.82 \cdot 10^4$	$6.68 \cdot 10^4$
	A_2 [/s^{-1}]	$1.7 \cdot 10^{12}$	$1.19 \cdot 10^{12}$	$1.53 \cdot 10^{12}$	$4.26 \cdot 10^{12}$
	E_2 [/(J/mol)]	$2.01 \cdot 10^5$	$1.96 \cdot 10^5$	$2.01 \cdot 10^5$	$1.85 \cdot 10^5$

The set of parameters based on the gas release for CO, CO_2 and CH_4 are approximately in the same range for all starting values. The obtained parameter sets, when optimizing for the SO_2 release, differ. This can also be seen from figure 27 where the reaction kinetics (average of the three sets A1, A2 and B2) for the four gas species and for the initial parameters is given.

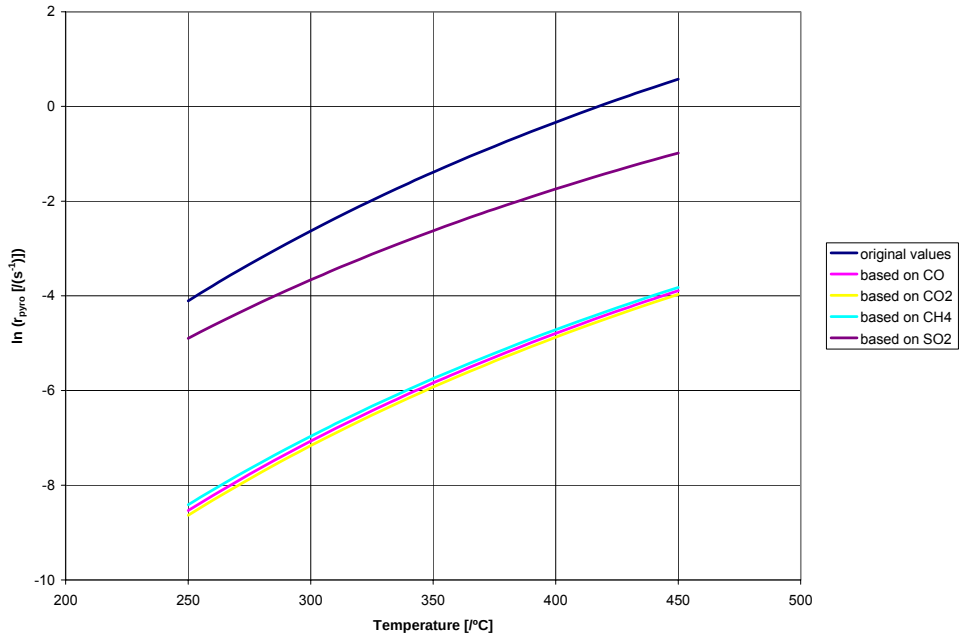

Figure 27: Optimized reaction kinetics at 375 °C

The initially used kinetic parameters that are based on devolatilization of coal give too high values for all species. The kinetics based on the three species CO, CO_2 and CH_4 are in the same range, whereas the resulting kinetics based on SO_2 are higher. It is important to state that these are the optimized values at 375 °C and might differ for other temperatures.

In order to see the improvements on the release data for the original program, the two sets A1 and A2 of parameters for the optimization based on CO where used. Figures 28 to 31 represent the four released species resulting from the original parameters, the two sets of optimized kinetic parameters and the experimental data.

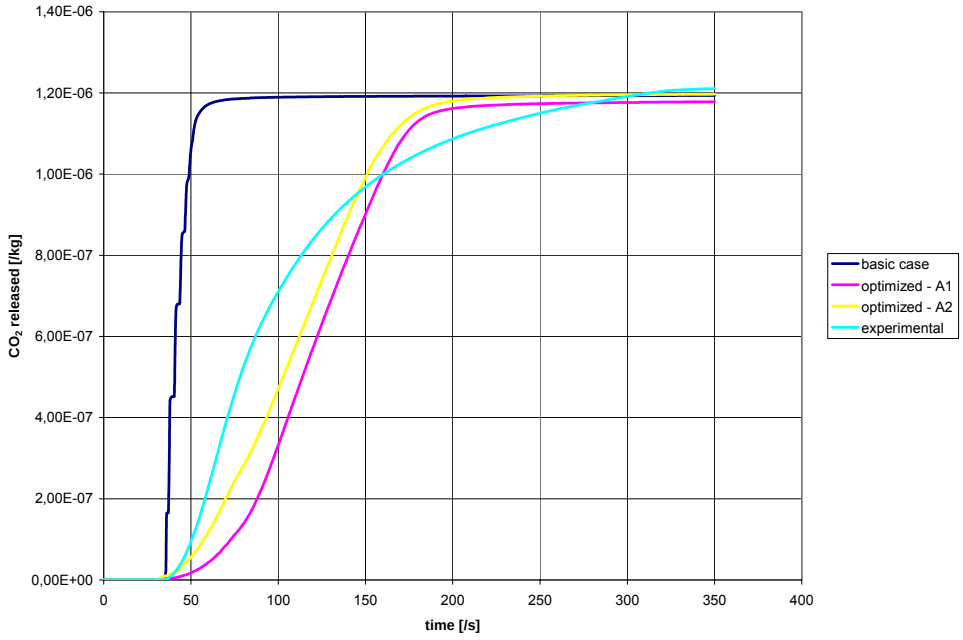

Figure 28: CO_2 release data for 375 °C

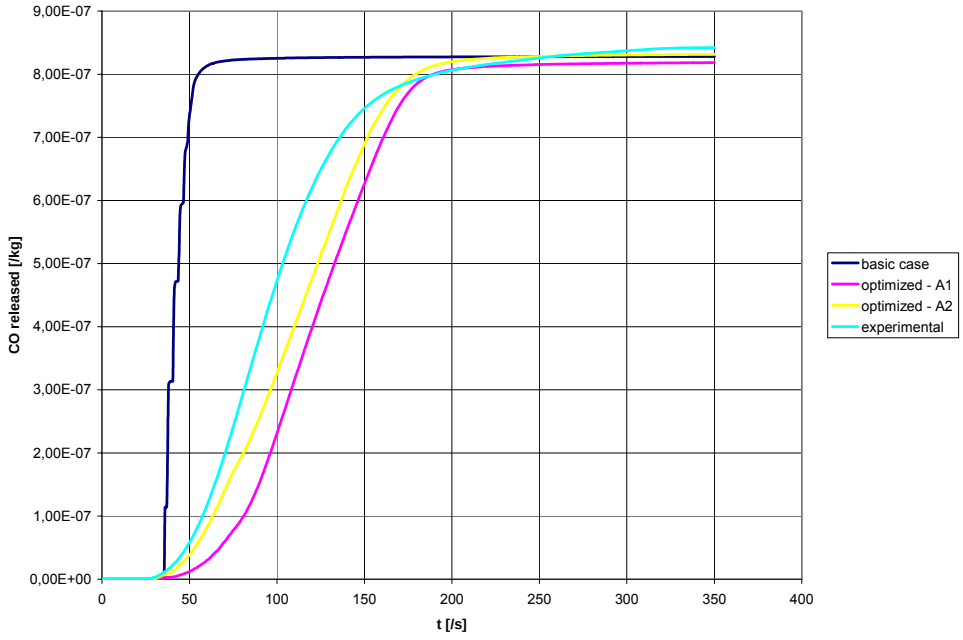

Figure 29: CO release data for 375 °C

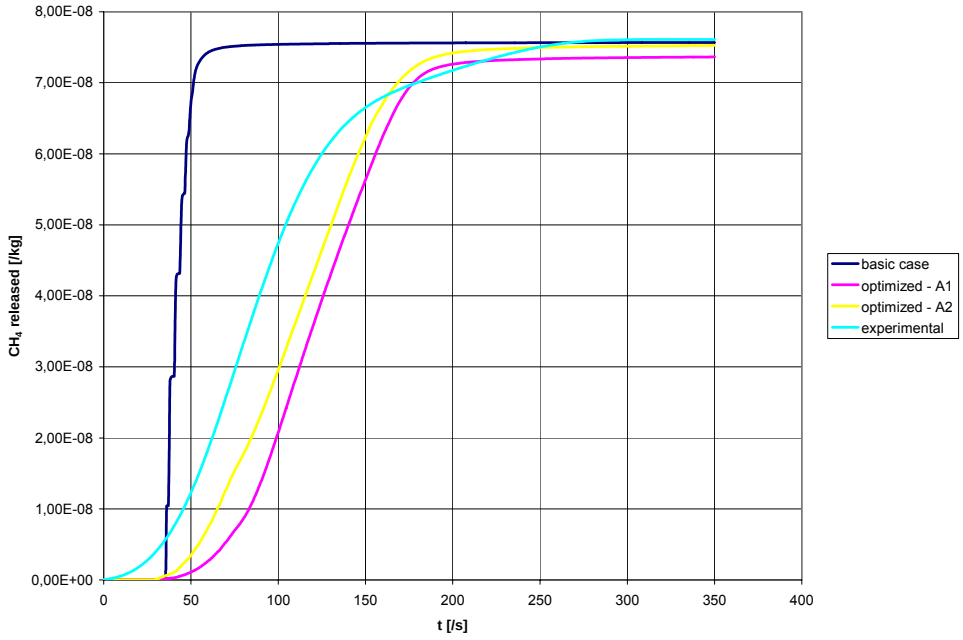

Figure 30: CH_4 release data for 375 °C

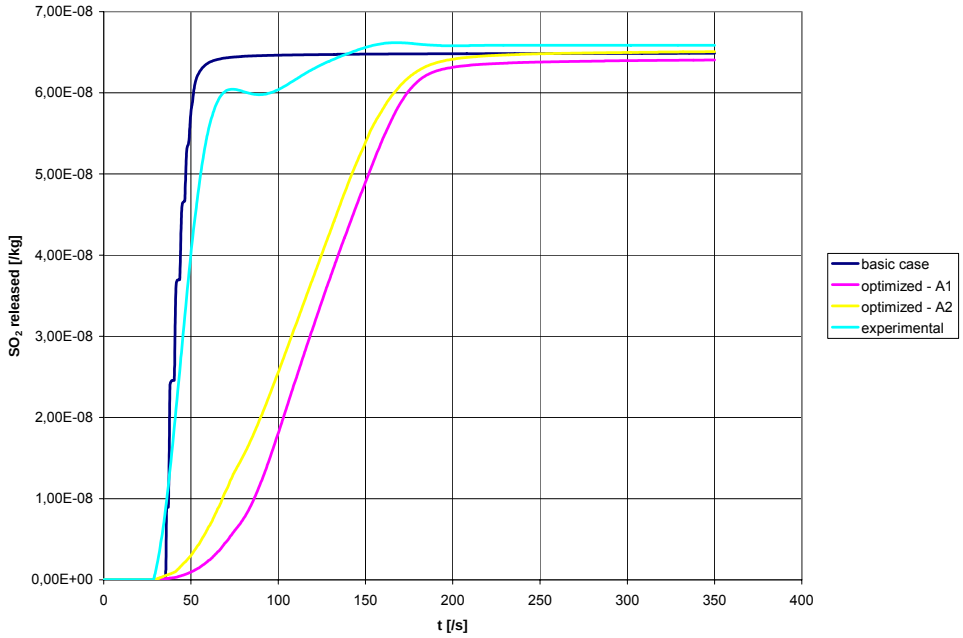

Figure 31: SO_2 release data for 375 °C

It can be clearly seen that the change in parameters improved the fit of the curves for CO_2, CO and CH_4 substantially. As already could be noticed in figure 27 the reaction kinetics based on CO are too low for the SO_2 release and therefore the fit is worst for this gas species. In the case of SO_2, the initial

parameters gave better fit than the optimized expression. But for the other three species, the CO based optimized kinetics gave an acceptable fit. The parameter set A2 assuming only one reaction even gives better fit for the temperature of 375 °C. That both optimized curves are resulting in a slower release of the gases compared to the experiments is caused by the simplification of the program used for the optimization, which – as already mentioned - is adjusting all gas release within the droplet to the experimental data. Perfect fit to the curves cannot be expected though, in particular as there are several other factors influencing the resulting gas release as well. One major factor is the temperature profile. As the simulated and experimental gas release each are based on the simulated, respectively the measured temperature profile, differences between the two profiles result in differences for the gas release. To illustrate that difference, the temperature profiles for both cases are given at 375 °C. The thin lines represent the temperature in the different sections for the simulation whereas the thick lines are the simulation average on one hand and the average of all experiments at 375 °C used for the evaluation on the other hand.

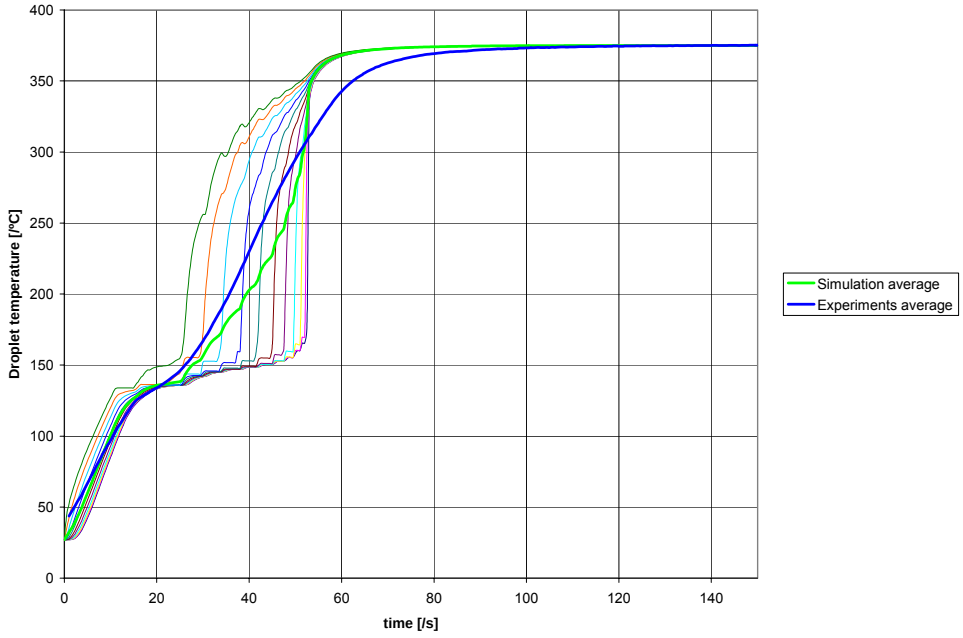

Figure 32: Temperature profiles at 375 °C - Simulation and Experiments

The difference is not too big, but as the resulting reaction kinetics are directly based on the temperature the influence cannot be neglected. Also, the mass transfer inside the droplet is significantly influencing the resulting gas release. All these properties are dependent on the physical properties and boundary conditions defined for the simulations.

The same optimization procedure was applied for a temperature of 400 °C. Only the three starting guesses that gave good and realistic results, namely A1, A2 and B1, were used in this case. Again, it can be seen that the resulting kinetics are in the same range for the three species CO, CO_2 and CH_4 but are higher and closer to the initially used coal kinetics for SO_2. For the first three species the kinetics are in the same range as for 375 °C (dashed lines in figure 33) whereas for SO_2 the kinetics are lower at 400 °C than they are at 375 °C.

Table 11: Kinetic parameter sets for optimization based on different gas species release data at 400 °C

		CO	CO_2	CH_4	SO_2
A1	A_1 [/s^{-1}]	$2.87 \cdot 10^5$	$2.98 \cdot 10^5$	$2.92 \cdot 10^5$	$3.24 \cdot 10^5$
	E_1 [/(J/mol)]	$9.67 \cdot 10^4$	$9.63 \cdot 10^4$	$9.63 \cdot 10^4$	$8.79 \cdot 10^4$
	A_2 [/s^{-1}]	$1.16 \cdot 10^{13}$	$1.21 \cdot 10^{13}$	$1.17 \cdot 10^{13}$	$1.28 \cdot 10^{13}$
	E_2 [/(J/mol)]	$2.91 \cdot 10^5$	$2.81 \cdot 10^5$	$2.88 \cdot 10^5$	$2.77 \cdot 10^5$
A2	A_1 [/s^{-1}]	15.24	13.86	15.87	45.48
	E_1 [/(J/mol)]	$4.31 \cdot 10^4$	$4.26 \cdot 10^4$	$4.29 \cdot 10^4$	$4.21 \cdot 10^4$
B1	A_1 [/s^{-1}]	$2.42 \cdot 10^4$	$3.63 \cdot 10^4$	$3.10 \cdot 10^4$	$4.26 \cdot 10^3$
	E_1 [/(J/mol)]	$8.34 \cdot 10^4$	$8.50 \cdot 10^4$	$8.42 \cdot 10^4$	$7.07 \cdot 10^4$
	A_2 [/s^{-1}]	$2.88 \cdot 10^{12}$	$1.78 \cdot 10^{12}$	$3.44 \cdot 10^{12}$	$5.04 \cdot 10^{12}$
	E_2 [/(J/mol)]	$2.09 \cdot 10^5$	$2.05 \cdot 10^5$	$2.08 \cdot 10^5$	$1.78 \cdot 10^5$

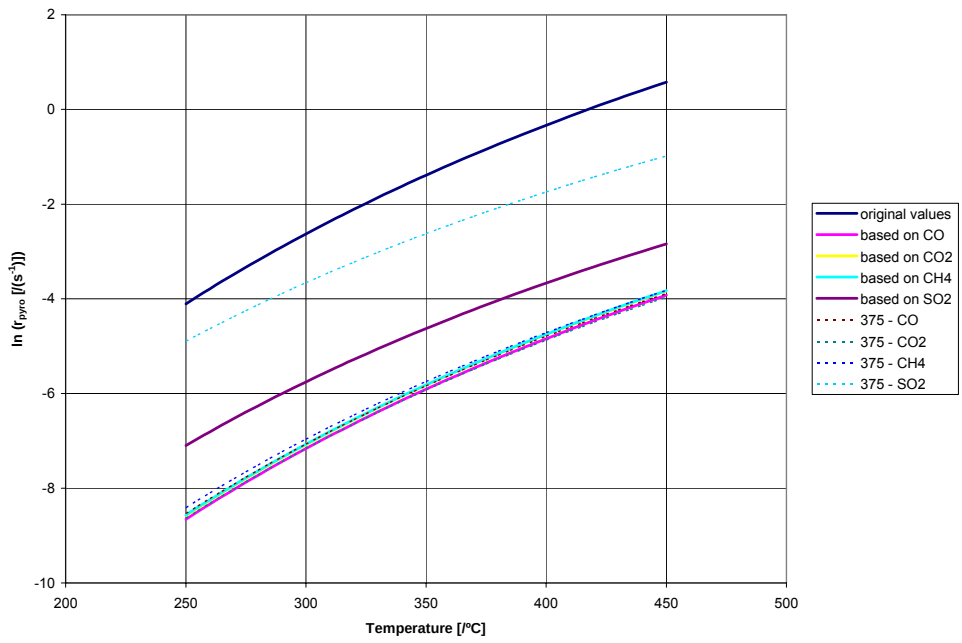

Figure 33: Optimized reaction kinetics at 400 °C

In next step, the optimized parameters based on CO at 375 °C and 400 °C where used for a calculation at 400 °C. Both parameter sets A1 and A2 were used. The ratio of gas release and the limit for the amount of solids to be pyrolysed was adjusted to the experimental values as given in table 5. Figures 34 to 37 clearly show that the parameters for 375 °C give a good fit at 400 °C as well. Even for SO_2, where the reaction kinetics showed some difference, the fit is almost the same as with the parameters at 400 °C.

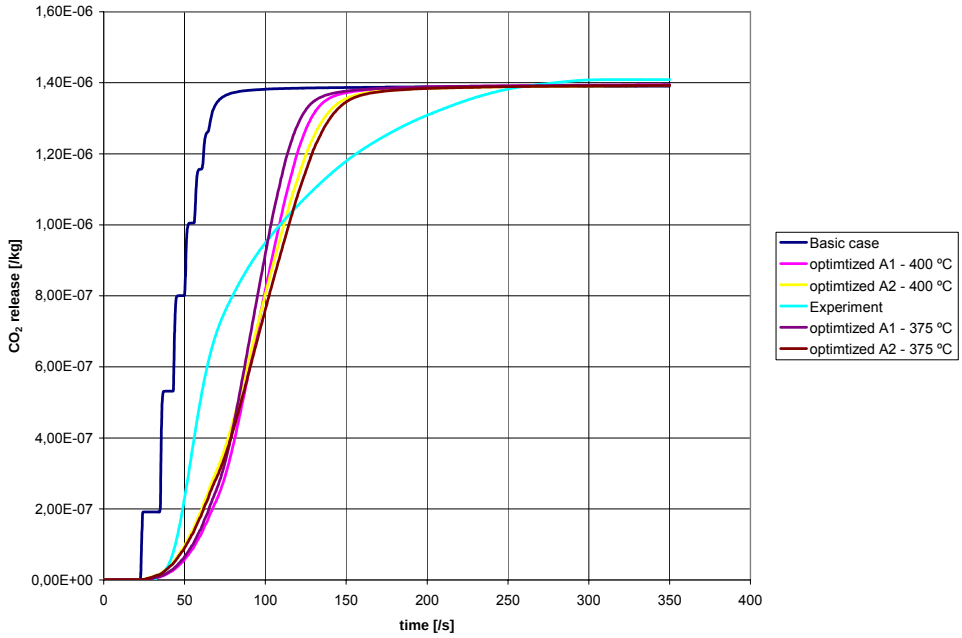

Figure 34: CO_2 release data for 400 °C

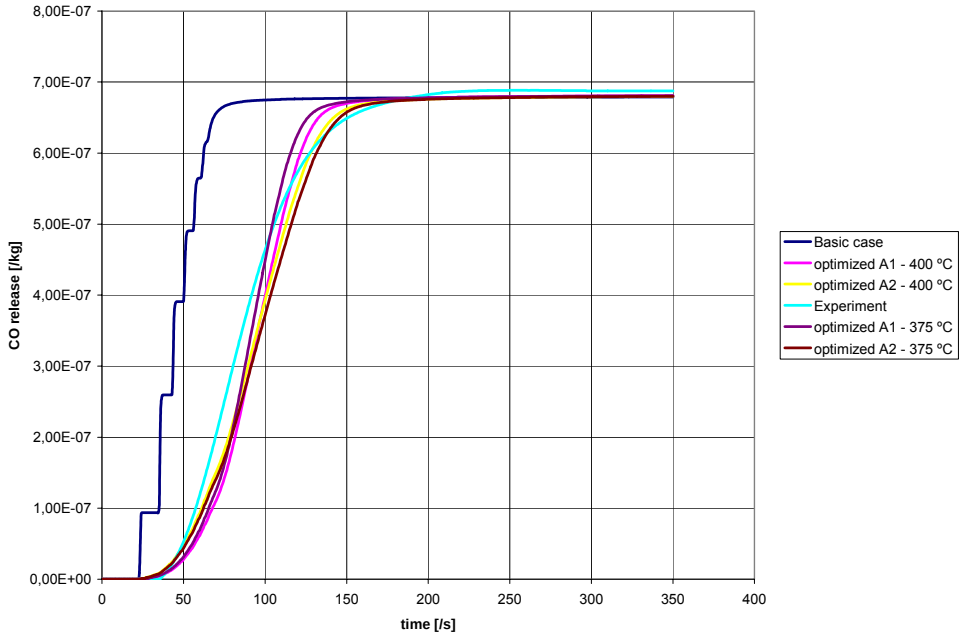

Figure 35: CO release data for 400 °C

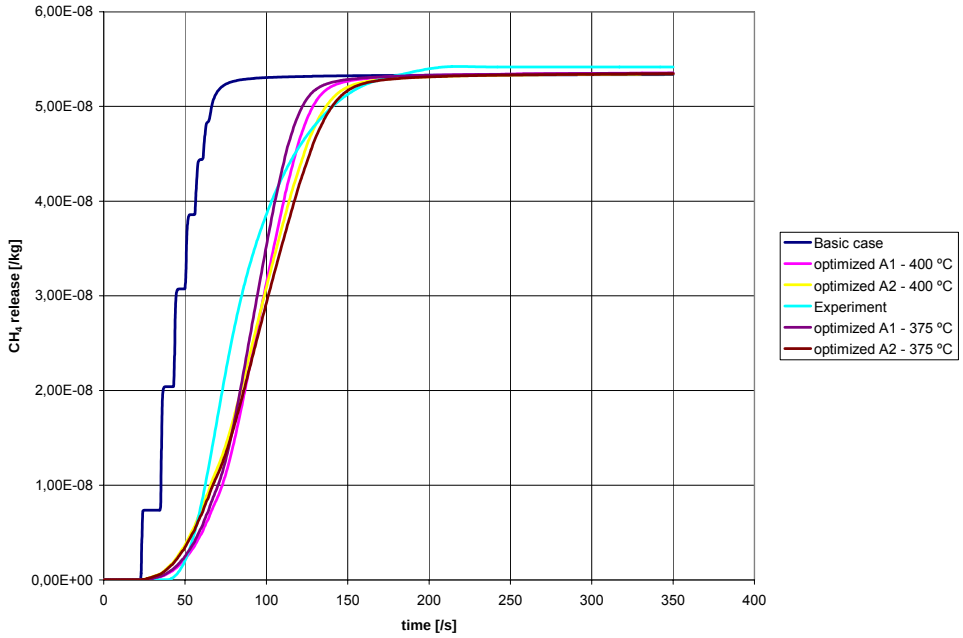

Figure 36: CH_4 release data for 400 °C

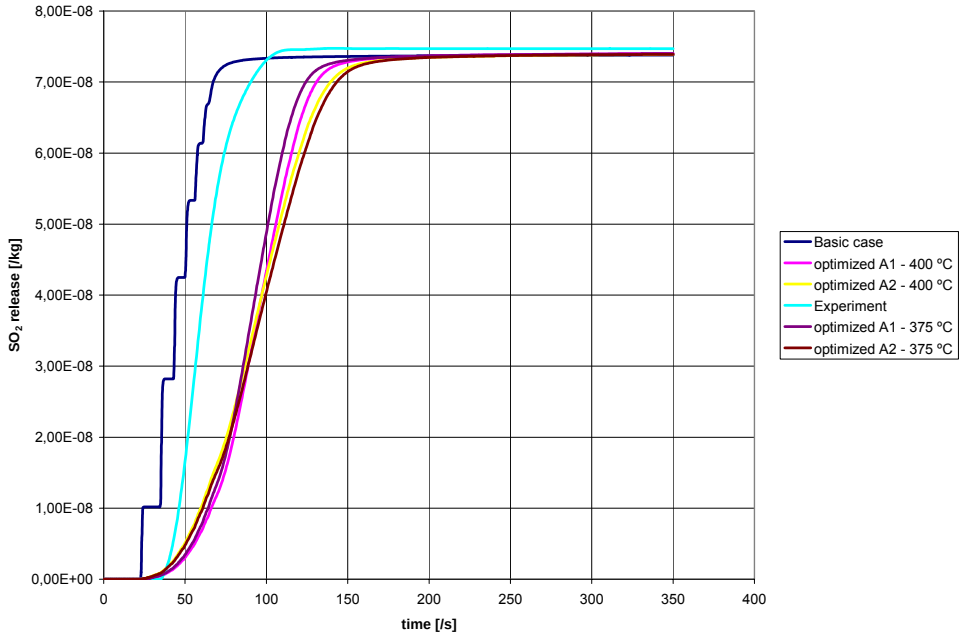

Figure 37: SO_2 release data for 400 °C

Finally it was tried to have one separate reaction for each species, resulting in 8 kinetic parameters. This was done for 375 °C and the obtained fit was less accurate than having one reaction for all species and using the release ratio obtained from the experiments. In particular for the species SO_2 the fit was worst. This is mainly due to the fact that it only is possible to limit the overall release of gases in this case, whereas it is possible to define the ratio of released gases when using one reaction for all species. The plots for the simplified program are given in figure 38

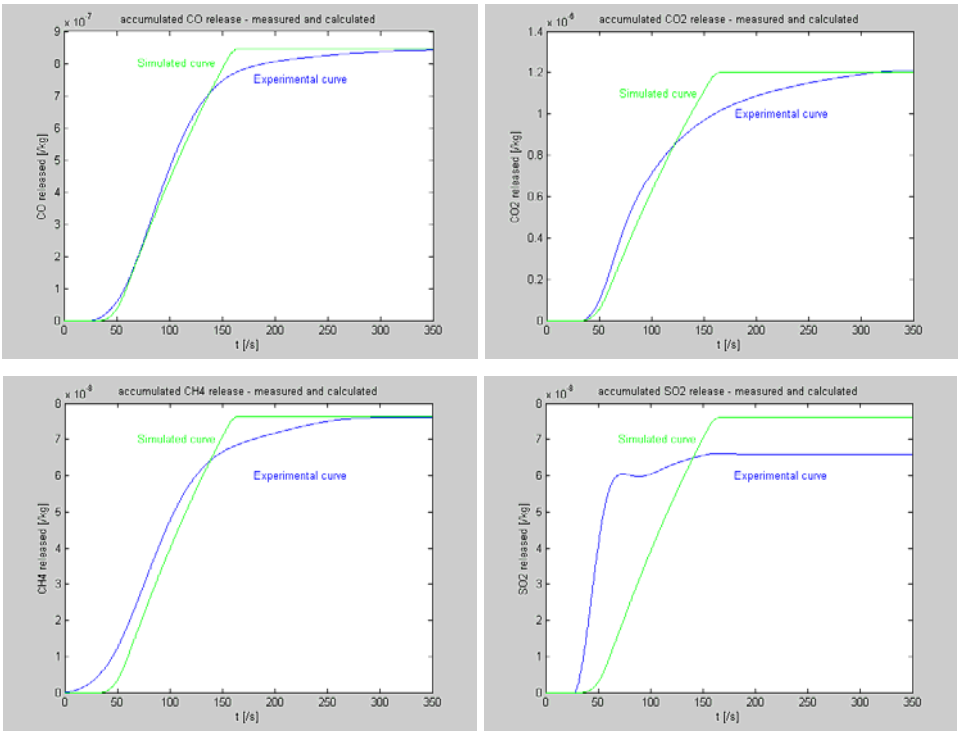

Figure 38: Fit between experimental and optimized gas release at 375 °C

The parameters obtained from that optimization were used for calculations at 375 and 400 °C to see if the change in release ratio can be simulated with the reaction kinetics obtained at 375 °C.

Table 12: Parameters obtained when assuming a single reaction for each species at 375 °C

Gas species	A_1 [/(s^{-1})]	E_1 [/(J/mol)]
CO	20.73	$5.05 \cdot 10^4$
CO_2	14.43	$4.67 \cdot 10^4$
CH_4	1.19	$4.80 \cdot 10^4$
SO_2	13.27	$6.10 \cdot 10^4$

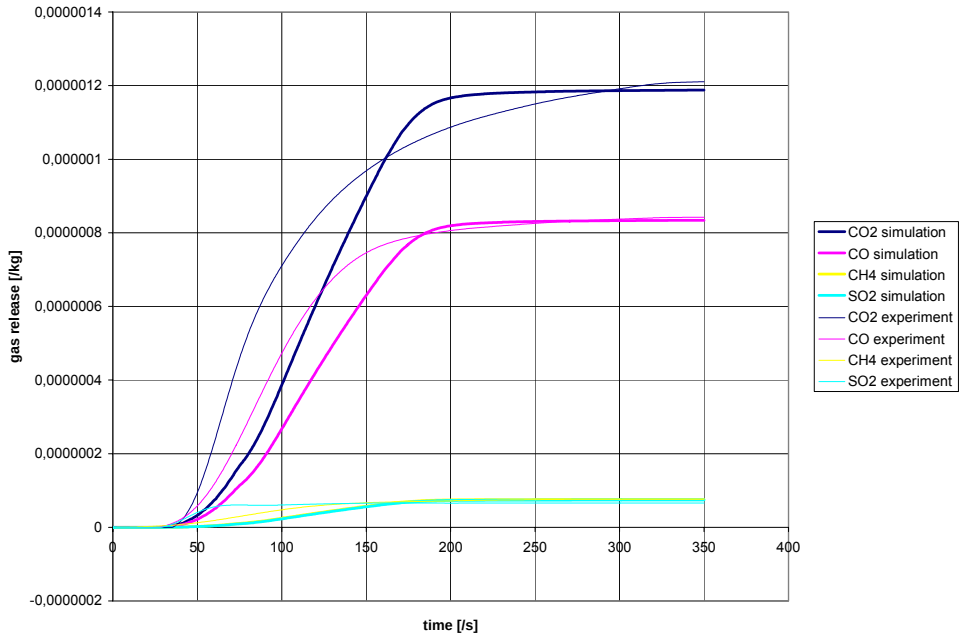

Figure 39: Simulated and experimental gas release at 375 °C using one reaction for each species

In figures 39 and 40 it can be seen that the kinetics obtained by optimization at 375 °C give an acceptable fit for this temperature. It is less accurate than using one or two reactions and the ratio of released gases though. For 400 °C the resulting release does not fit to the experimental results. It therefore is not possible to implement pyrolysis kinetics for each species describing the release correctly over a broad temperature range. This is probably due to the fact that each species is produced by several reactions from the organic material therefore making it hard to describe the release with a single reaction.

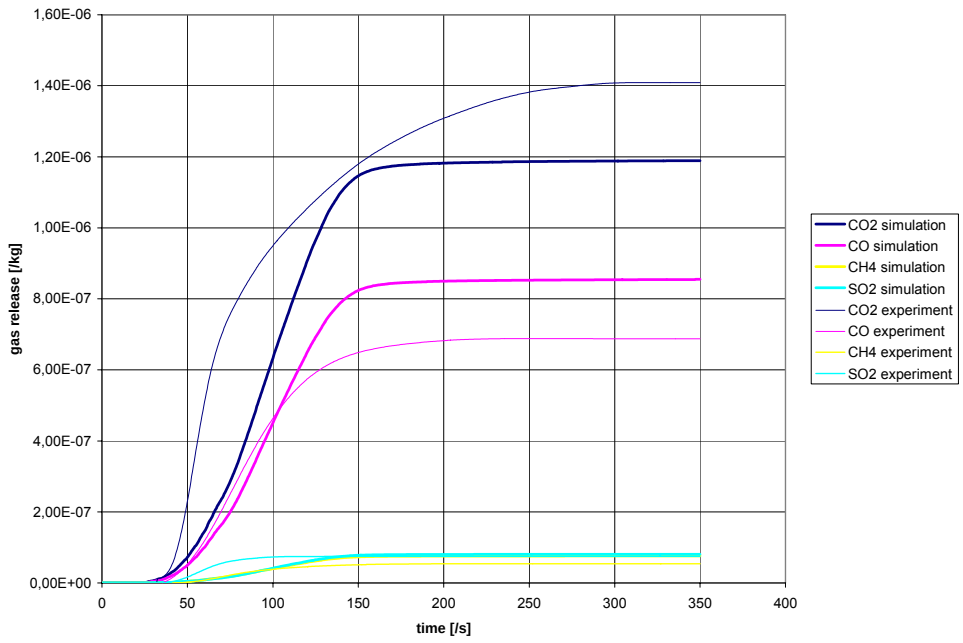

Figure 40: Simulations at 400 °C with 8 parameters obtained at 375 °C

Conclusions

In the optimization part, it has been found that it is possible to adjust the kinetic parameters with help of experimental data. The MATLAB program, used for the simulations, has been extended, now being able to handle different gas species. This can easily be extended to more than the five species H_2O, CO_2, CO, CH_4 and SO_2 that are included at the moment. The heat transfer modelling has been changed to a more advanced model based on the dusty gas model for porous media. The experiments performed in the range of 275 to 400 °C gave results with high fluctuations. The dry solid mass loss can be expected to be between 20 and 40 %. An elemental analysis at 400 °C indicates a dry mass loss of about 27 %. At 375 and 400 °C, the four measured gases during the experiments account for about 20 to 40 % of all gases released during pyrolysis. The two main released gases are CO and CO_2 and the ratio of the gases changes for the different temperatures. The onset of pyrolysis reactions has been assumed to be at 300 °C which was in accordance with the experiments.

A method to find optimized kinetic parameters has been developed using a simplified program. The resulting kinetics are lower than the initially ones based on devolatilization of coal. For the three species CO, CO_2 and CH_4, the kinetics were in the same range for both 375 and 400 °C. When optimizing the kinetics based on the experimental data for SO_2, higher reaction kinetics were obtained and in addition these kinetics differed for 375 and 400 °C. The reason for this might be that the pyrolysis reactions for SO_2 are faster than for the other species, but could also be due to the uncertainties implied in method of deconvolution, in particular in case of low gas release as for SO_2. The fit between the simulated and experimental curves was improved substantially by the optimized kinetics and even the kinetics obtained at 375 °C gave good fit at 400 °C. In the examined temperature range, it is possible to replace the two parallel reactions by only one reaction without losing accuracy in the fit of data. It was not possible to get an acceptable fit for the gas release using one reaction for each species. By defining the ratio of gases released at each temperature, it is possible though to get good fit to the experimental data with one set of kinetics.

Recommendations

During the experiments it was found that the measurement of the mass of the droplet still needs to be improved. To properly estimate the mass loss in the experiments it is necessary to determine the final mass of the pyrolysed droplet. By that it also is possible to get a better idea about the amount of gases that are produced but not measured. The gas measurements themselves also gave strange results and it is questionable if the method of deconvolution can be properly applied on the existing equipment as the dead-time of the analysers is quite high.

In order to further investigate if the obtained kinetics fit the experimental data, it is necessary to check for higher temperatures. An interesting aspect here is to see if the different behaviour of SO_2 release can be confirmed for a higher temperature range or if the difference only is due to a high uncertainty of the

deconvolution process at low concentrations. Another important aspect to ensure more reliability of the obtained kinetics is to verify the physical properties of black liquor that are used in the program. Properties like surface tension, viscosity or heat capacity are influencing the swelling behaviour and the heat transfer, and will therefore influence the temperature profile and, consequently, the gas release. Here, it is important to take into account the gases that are released, but not measured, in the simulations as the gas release determines the swelling. It might also be useful to test the grid independence by changing the number of cells used for the calculations. Depending on the size of the droplet the assumption of equal conditions within one section might be questionable. Finally it might be necessary to have several optimization runs for the kinetic parameters as a change in the gas release will cause a change in the temperature profile. Preliminary examinations though showed that the difference is minimal and can be neglected compared to other sources of error.

Reference List

[1] JÄRVINEN, M.P., 2002, Numerical Modelling of the Drying, Devolatilization and Char Conversion Processes of Black Liquor Droplets, *Acta Polytechnica Scandinavica*, Mechanical Engineering Series No. 163, Espoo

[2] Skogsindustrierna – Swedish Forest Industries Federation, Publications and Surveys – In balance with nature – *The vision becomes reality*, http://www.forestindustries.se/eng/balans/verklig.htm, 2005-01-25

[3] HARVEY, S., FACCHINI, B., 2004, Predicting black liquor gasification combined cycle powerhouse performance accounting for off-design gas turbine operation, *Applied Thermal Engineering,* Vol. 24, pp. 111-126

[4] ADAMS, T.A. (Editor), 1997, *Kraft Recovery Boilers,* TAPPI Press, Atlanta, Canada

[5] ANTAL, M.J., VÁRHEGYI, G., JAKAB, E., 1998, Cellulose Pyrolysis Kinetics: Revisited, *Industrial & Engineering Chemistry Research,* Vol. 37, pp. 1267-1275

[6] CORDERO, T., RODRÍGUEZ-MAROTO, J.M., RODRÍGUEZ-MIRASOL, J., RODRÍGUEZ, J.J., 1990, On the kinetics of thermal decomposition of wood and wood components, *Thermochimica Acta,* 164, pp. 135-144

[7] CABALLERO, J.A., FONT, R., MARCILLA, A., 1996, Study of the primary pyrolysis of Kraft lignin at high heating rates: yields and kinetics, *Journal of Analytical and Applied Pyrolysis*, Vol. 36, pp. 159-178

[8] FERDOUS, D., DALAI, A.K., BEJ, S.K., THRING, R.W., 2002, Pyrolysis of Lignins: Experimental and Kinetics Studies, *Energy & Fuels,* Vol. 16, pp. 1405-1412

[9] UBHAYAKAR, S.K., STICKLER, D.B., VON ROSENBERG, C.W., GANNON, R.E., 1976, Rapid Devolatilization of Pulverized Coal in Hot Cumbustion Gases, *16th International Symposium on Combustion,* pp. 427-436

[10] MERRIAM, R.L., 1980, Kraft, version 2.0: Computer model of kraft recovery furnace. *American paper institute,* Cambridge, MA

[11] SHICK, P.E., 1986, Predictive simulation of recovery furnace processes on a microcomputer, *Tappi 1986 Recovery Operations Seminar,* Orlando, FL, pp. 121-133

[12] KULAS, K.A., 1990, *An overall model of the combustion of a single black liquor droplet of kraft black liquor,* Doctoral thesis, Institute of Paper Science and Technology, USA

[13] FREDERICK, W.J., 1990, *Combustion Processes in Black Liquor Recovery: Analysis and Interpretation of Combustion Rate Data and Engineering Model,* DOE Report DOE/CE/40637-T8, USA

[14] THUNMAN, H., 1994, Combustion of black liquor droplets in a recovery boiler (In Swedish: Förbränning av svartlutsdroppar i en sodapanna), Chalmers University of Technology, Sweden

[15] HARPER, F.D., 1989, *Sulfur release during the pyrolysis of kraft black liquor,* Doctoral Thesis, Institute of Paper Chemistry, USA

[16] MANNINEN, J., VAKKILAINEN, E., 1996, *Reduction of Sulphur emissions from kraft recovery furnace with black liquor heat treatment*, 29th Latin American Congress for Pulp and Paper. Sao Paulo, Brasilia, Associacao Brasileira Technica de Celulose e Paper

[17] SAASTAMOINEN, J.J., 1996, Modelling of drying, devolatilization and swelling of black liquor droplets, *AIChE Symposium Series 92*: 311 74

[18] VERRIL, L.V., WESSEL, A.R., 1995, Sodium Loss During Black Liquor Drying and Devolatilization – Application of Modeling Results to Understanding Laboratory Data, *1995 International Chemical Conference,* Toronto, Ontario, Canada, Tappi Press, Atlanta, pp. B89-B103

[19] CHASE, G.G., MAIER, E., 2003, Filtration – 6. Cake Filtration Theory, *Kirk-Othmer Encyclopedia of Chemical Technology*, John Wiley & Sons Inc., http://www.mrw.interscience.wiley.com/kirk/articles/filtsvar.a01/sect6-fs.html, Electronic book (2005-02-25)

[20] MÖRSTEDT, S.-E., HELLSTEN, G., 2003, *DATA OCH DIAGRAMM – Energi- och kemitekniska tabeller,* Liber AB, Stockholm, Sweden

[21] SAASTAMOINEN, J., RICHARD, J.-R., 1996, Simultaneous Drying and Pyrolysis of Solid Fuel Particles, *Combustion and Flame*, Vol. 106, pp. 288-300

[22] JÄRVINEN, M.P., ZEVENHOVEN, R., VAKKILAINEN, E., FORSSEN, M., 2003, Effective thermal conductivity and internal thermal radiation in burning black liquor particles, *Combustion Science and Technology,* Vol. 175(5), pp.873-900

[23] LILIEDAHL, T., SJÖSTRÖM, K., WIKTORSSON, L.-P., 1991, Analysis Method of Pyrolysis Kinetics Using Modern Singal Processing Techniques, *American Institute of Chemical Engineers (AIChE) Journal*, Vol. 37(9), pp.1415-1419

[24] EDGAR, T.F., HIMMELBLAU, D.M., LASDON, L.S., 2001, *Optimization of chemical processes*, 2nd edition, McGraw-Hill, Boston, USA

List of Symbols

Standard symbols

a_R	[m^{-1}]	Rosseland mean absorption coefficient
A	[m^2]	area
A_1.A_2	[s^{-1}]	collision frequency factors for pyrolysis
C_P	[J/(kg·K)]	heat capacity
DC	[-]	dry content
E_1.E_2	[J/mol]	activation energies for pyrolysis
k	[W/(m·K)]	thermal conductivity
m	[kg]	mass
$\dot{m}$	[kg/s]	mass flow
M	[kg/mol]	molar mass
P	[Pa]	pressure
q	[J]	energy
r	[m]	radius
T	[K]	temperature
tstep	[s^{-1}]	inverse of time step
V	[m^3]	volume

Greek symbols

Δ	[-]	difference
ϕ	[-]	porosity
μ	[Pa·s]	dynamic viscosity
ρ	[kg/m^3]	density

Indices

0	initial
acc	accumulated
BL	black liquor
boil	boiling
bub	bubble
E	excess
evap	evaporation
G	gases
i	intersectional
in	coming in
inc	increase
new	new (at the next time step)
old	old (at the current time step)
out	leaving
pyro	pyrolysis
S	solids
W	water

Constants

K	Darcy constant	10^{-5}	[m]
R	gas constant	8.314	[J/(mol·K)]
ε	emissivity factor for black liquor	0.562	[-]
π	Pi	3.14	[-]
σ	Stefan-Boltzmann constant	$5.67 \cdot 10^{-8}$	[W/(m^2·K^4)]

Appendix A – Matlab program code

Main program – blg2.m

Latest version of the main program with the optimized parameter set for 375 °C.

```
% Calculates the black liquor swelling during drying, pyrolysis and
% gasification

clear all      % clear memory
tic            % start "stop watch"

% physical properties of black liquor
Cps = 1000;          % heat capacity BLS [J/kg,K]
rho = 1200;          % density [kg/m3]
DC = 0.64;           % dry content
viskbl=1e5;          % viscosity of black liquor [Pa·s]
surfbl=0.2;          % surface tension of black liquor [N/m]
Kawater=2;           % darcy constant for BL during drying/evaporation
Kapyrol=6e-5;        % darcy constant for BL during pyrolysis
eps0 = 0.01;         % initial porosity of BL

% other physical properties (water/gases)
h=57.4;                  % outer heat transfer coefficient [W/m2]
Cpg = 100;               % heat capacity (gases) [J/kg,K]
Cpw = 4180;              % heat capacity water   [J/kg,K]
dHevap = 2245000;        % evaporation energy [J/kg]
visk = 5e5;              % viscosity of produced gases [Pa·s]
kgas = 0.3;              % heat conductivity of the gases [W/m,K]
M_H2O = 0.018;           % [kg/mol] The gas G is represented by 7 different
M_CO = 0.028;            % [kg/mol] compounds H20, CO, CO2, CH4, SO2, H2S, N2
M_CO2 = 0.044;           % [kg/mol] G is the overall gas mass
M_CH4 = 0.016;           % [kg/mol]
M_SO2 = 0.064;           % [kg/mol]
M_H2S = 0.034;           % [kg/mol]
M_N2 = 0.028;            % [kg/mol]

% pyrolysis kinetics data:
A1 = 3.46e5;             % rate coeff. [1/s]
E1 = 9.7e4;              % activation energy [J/mol]
A2 = 1.33e13;            % rate coeff. [1/s]
E2 = 2.6e5;              % activation energy [J/mol]
dHpyro = 1.45e5;         % heat of react. [J/kg BLS]

% general constants
emm = 0.56;              % emission coefficient [-]
sigma_rad = 5.67e-8;     % Stefan-Boltzmans constant [W/m2,K4]
Rg = 8.3145;             % gas constant [J/mol,K]
aR = 850;                % Rosseland mean adsorption coefficient [1/m]
% input data
Tsurr = 273+375;         % surrounding temperature [K]
```

```
Tdrop = 300;            % droplet temperature [K]
Tpyro = 573;            % temperature when pyrolysis starts [K]
Psurr = 101325;         % surrounding pressure in the reactor [Pa]
d0 = 4.2e-3;            % droplet diameter
n = 10;                 % number of intervalls for the sectioning of the droplet
nbubble = 1000000;      % number of gas bubbles inside droplet overall
tstep = 100;            % time steps [1/s]
sim_time = 350;         % simulation time [s]

amax = 1;
maxiter = 0;
counter = 0;
time = tstep*sim_time;   % time for simulation [1/tstep]

% Initialization
% V0 = volume (m3)
% W0 = amount of liquid water (kg)
% S0 = amount of solids (kg)
% G0 = overall amount of gases  (kg)

% Dividing the droplet in sections

% Overall volume of the droplet
Vtot=4*pi/3*(d0/2)^3;
% First section - inner sphere r = 0
r(1,1)=0;
% Section 2-n - inner "sphereshells"
for i =2:n
   r(1,i)=r(1,i-1)+d0/2/n;
end
% Section n+1 - outer "sphereshell"
r(1,n+1)=d0/2;

% Defining the radius for the intersection area ri(i)
% and the volume of each section V0(i)
for i = 1:n
   % for section 1 (inner sphere)
   if i == 1
      ri(i) = (((d0/2/n)^3)/2)^(1/3);
      V0(i) = 4*pi/3*ri(i)^3;
   % for section 2-6 (inner and outer sphereshells)
   else
      ri(i) = ((r(i+1)^3+r(i)^3)/2)^(1/3);
      V0(i) = 4*pi/3*ri(i)^3-4*pi/3*ri(i-1)^3;
   end
   % number of bubbles per section
   nbub(i) = round(V0(i)*nbubble/Vtot);
   if nbub(i) == 0
      display('to low number of bubbles')
      pause
   end
   % Radius of the bubbles in each section - void bubble size
   Rbub(i) = (3/4/pi*V0(i)*eps0/nbub(i))^(1/3);
end
```

```
% put the calculation points in the middle of the calculations cells
% which are defined by ri not r. 1 and n+1 will not change.
for i = 2:n
   r(1,i) = ((ri(i)^3+ri(i-1)^3)/2)^(1/3);
end

% Volume, number of bubbles and void bubble size for the outer section
V0(n+1) = Vtot-4*pi/3*ri(n)^3;
nbub(n+1) = round(V0(n+1)*nbubble/Vtot);
Rbub(n+1) = (3/4/pi*V0(n+1)*eps0/nbub(n+1))^(1/3);

%initial bubble radius
Rbubstart = Rbub;

% initial water amount of each section
W0(1:n+1) = V0*rho*(1-DC);
% initial solid amount of each section
S0(1:n+1) = V0*rho*DC;
% initially the gas inside the droplet is assumed to be N2 as the working atmosphere is N2
G0(1:n+1) = eps0*V0'*Psurr/Rg/Tdrop*M_N2;
% initial temperature of each section
T0(1:n+1) = Tdrop;
% initial pressure of each section
P0(1:n+1) = Psurr;
% volume for time step 1 for each section
V(1,:) = V0;
% water amount for time step 1 for each section
W(1,:) = W0;
% solid amount for time step 1 for each section
S(1,:) = S0;
% thermal conductivity for all sections (only initialisation values - will be calculated)
k(1,1:n+1) = 0.1;
% gas amount for time step 1 for each section
% initially there is only N2 in the gas phase of the bubbles
% seven components are taken into account H2O, CO, CO2, CH4, SO2, H2S & N2
% they are released during evaporation (H2O) and pyrolysis
for x = 1:n+1
   G(1,x,1:7) = [0 0 0 0 0 0 G0(x)];
end
% released gases for time step 1
Gas_released(1,:) = [0 0 0 0 0 0 0];
% temperature for time step 1 for each section
T(1,:) = T0;
% pressure for time step 1 for each section
P(1,:) = P0;
% accumulated released gases at time step 1
ARG(1) = 0;
% accumulated released gases component-specific at time step 1
ACC_GAS(1,1:7) = 0;
% initial mass of drop (kg)
m_o_d(1) = sum(V0*rho);
% porosity for each section
eps(1,1:n+1) = eps0;
% evaporated water in each section
H2O_vap(1,1:n+1) = 0;
```

```
% Dummy values for porosity, radius, intersection area radius and bubble
% void radius
eps_new = eps;
rnew = r;
rinew = ri;
Rbubnew = Rbub;

% first evaporation will occur - so Darcy constant set to this value
Ka = Kawater;

% calculations
tmax=time/tstep;
t = 0;
t0=1;
time_s = 0;
tstep0 = tstep;
t_crit = 0;
while time_s <= sim_time
% for t=1:time
   % simulation time is increased by time step
   time_s = time_s + 1/tstep;
   time_s = round(time_s*10000)/10000;
   t = t + 1;
   % counting up each second of the calculation time - display
   if time_s>t0
      disp([round(time_s),tstep,sim_time])
      t0=t0+1;
   end

   if t > t_crit + tstep/10 & tstep > tstep0 & mod(time_s,2.0/tstep) == 0
   % 64 is used to keep "good" steps
      tstep = tstep/2;
      t_crit = t;
   end
   % guessed pressure in the cells at t+1
   Pguess(1:n+1) = P(t,1:n+1);
   % dummy value
   Pnew(1:n+1) = P(t,1:n+1);
   % pressure change check - when it is lower than 0.002 the pressure is accepted as correct
   condition = 1.0;
   % variable to count the iterations during pressure calculation
   a = 0;
   while condition > 0.002  % iteration to find the right pressure
      ARG(t+1) = ARG(t);
      ACC_GAS(t+1,:) = ACC_GAS(t,:);
      H2O_vap(t+1,1:n+1) = H2O_vap(t,1:n+1);
      rnew = r(t,:);
      rinew = ri;
      % counting the number of iterations a
      a = a+1;
      % storing the maximum number of iterations
      if a > amax
         amax = a;
      end
```

```
if a > 40
% in case to many iterations are needed the time step is decreased
    % is just a testing value
    backstep = 1;
    % guessed pressure in the cells at t
    Pguess(1:n+1) = P(t-backstep,1:n+1);
    Pnew(1:n+1) = P(t-backstep,1:n+1);
    % back one time step
    time_s = timevec(t+1-backstep);
    % increase time step
    tstep = tstep*2;
    t_crit = t;
    % set back time calculator
    t = t-backstep;
    a = 0;
end
if tstep > 15000
  beep
  disp('to small time step');
  pause
end
% this is a simple adaptation but might have to be modified for better speed
Pguess=0.2*Pnew+0.8*Pguess;

% calculation for each section
for x=1:n+1
    % mass and energy balances
    if x==1         % inner section
        % the energy "leaving" through the point "0" - the centre of the droplet -
        % will still be in that sectionso no energy can go out
        out(1)=0;
        % the same applies for the gas
        gas_out(1)=0;
    else
        % setting the energy & mass "in in the inner section" treated before
        out(x)=in(x-1);
        % equal to the energy & mass "out of the actual section"
        gas_out(x)=gas_in(x-1);
    end
    % using the right darcy constant for evaporation and pyrolysis
    if W(t,x) > 0
        Ka = Kawater;
    else
        Ka = Kapyrol;
    end

    % outer section
    if x==n+1
        % the average pressure in the outer section
        Pavg = (P(t,n+1)+Pguess(n+1))/2;
        % the flux of gas due to pressure difference according to Darcy's law
        vg = -Ka/visk*(Pavg-Psurr)*eps(t,x)^3/(1-eps(t,x))^2;
```

```
    % if the pressure in the outer section is higher than the surrounding pressure
    % the molar mass of the gas flowing out will be the one in this section
    if  vg <= 0
      Gas_vector(1:7) = G(t,x,1:7);
      M_avg = Molmass(Gas_vector);
    % else the gas flowing in will be N2 from the surrounding (simplification)
    else
      M_avg = M_N2;
    end
    % gas mass increase in kg
    gas_in(x) = 4*pi*rnew(x)^2*vg*Pavg/Rg/T(t,x)*M_avg/tstep;
    % amount of heat due to convection, radiation and the gas mass increase
    in(x) = 4*pi/tstep*rnew(x)^2*(h*(Tsurr-T(t,x)) +...
       emm*sigma_rad*(Tsurr^4-T(t,x)^4)) +...
       gas_in(x)*Cpg*(T(t,x)-273);
    % new mass of droplet
    m_o_d(t+1) = m_o_d(t)+gas_in(x);

% all other sections - inner sections
else
    % distance between the centre points of two neighbouring sections
    dr = rnew(x+1)-rnew(x);
    % temperature difference between two neighbouring sections
    dT = T(t,x+1)-T(t,x);
    % average pressure in the inner of the two section looked at
    Pavg1 = (P(t,x)+Pguess(x))/2;
    % average pressure in the outer of the two section looked at
    Pavg2 = (P(t,x+1)+Pguess(x+1))/2;
    % flux of gas between theses two sections
    vg = -Ka/visk*(Pavg1-Pavg2)*eps(t,x)^3/(1-eps(t,x))^2;
    % if the pressure in the inner section (x) is higher than the outer one (x+1)
    % the molar mass of the gas flowing out will be the one in the inner section
    if vg <= 0
      Gas_vector(1:7) = G(t,x,1:7);
      M_avg = Molmass(Gas_vector);
    % else the gas flowing in will be the one from the outer section
    else
      Gas_vector(1:7) = G(t,x+1,1:7);
      M_avg = Molmass(Gas_vector);
    end
    % dry content of the section under consideration
    St=S(t,x)/(S(t,x)+W(t,x));
    % correlation for the heat conduction of the solids
    ks(t,x) = (1.44*10^(-3))*(T(t,x)-273.15) + 0.58 - 0.335*St;
    % heat transfer inside the droplet
    k(t,x) = ks(t,x)*(1-eps(t,x)^(2/3)) + ...
       (eps(t,x)^(2/3))/((1-eps(t,x)^(1/3))/ks(t,x) + ...
       (eps(t,x)^(1/3))/kgas) + (16*sigma_rad*T(t,x)^3)/(3*aR)*eps(t,x);
    % gas mass increase in kg
    gas_in(x)=4*pi/tstep*rinew(x)^2*vg*eps(t,x)*Pavg1/Rg/T(t,x)*M_avg;
    % energy increase due to conduction and the gas mass increase
    in(x)=k(t,x)*4*pi/tstep*rinew(x)^2*dT/dr+gas_in(x)*Cpg*(T(t,x)-273);
end
```

```
% gas accumulation (mass transport) for the section under consideration
ack_gas(x) = gas_in(x)-gas_out(x);
% energy accumulation for the section under consideration
ack(x) = in(x)-out(x);
% dummy value
ack2 = ack(x);
% dry content of the section under consideration
St = S(t,x)/(S(t,x)+W(t,x));
% calculation of the heat capacities based on temperature and
% dry content -> function heatcap
[Cpw, Cps, CpE] = heatcap(T(t,x),St);
% boiling point calculation based on dry content
Tboil = 373+50*St.^2.74+101.06*(P(t,x)/1e5)^0.2487-101.39;

% E V A P O R A T I O N

% test if evaporation occurs: T above boiling point & water left to evaporate
if T(t,x) >= Tboil & W(t,x)>0
   % dummy value
   acktot = ack(x);
   % test to see if all is dried
   % assuming all water of the section being evaporated
   dW = W(t,x);
   % the new energy accumulation is reduced as energy is used for evaporation
   ack2 = acktot-dW*dHevap;
   % the new water amount is reduced by the amount evaporated
   % (is equal to zero in this case as all water is evaporated)
   W(t+1,x) = W(t,x)-dW;
   % the gas amount is increased by the mass of evaporated water
   G(t+1,x,1) = G(t,x,1) + dW;
   % overall gas mass [kg]
   GAS = G(t+1,x,1)+G(t,x,2)+G(t,x,3)+G(t,x,4)+G(t,x,5)+G(t,x,6)+G(t,x,7);
   % temperature change
   dT = ack2 / (S(t,x)*Cps + W(t+1,x)*Cpw + GAS*Cpg);
   % new temperature
   T(t+1,x) = T(t,x) + dT;
   % new dry content
   St = S(t,x) / (S(t,x) + W(t+1,x));
   % new boiling point
   Tboilnew = 373 + 50*St.^2.74+101.06*(P(t,x)/1e5)^0.2487-101.39;

   if T(t+1,x) < Tboilnew
   % Partial evaporation occurs as the new temperature obtained by the assumption
   % that all water is evaporated is lower than the the real boiling point
   % for complete evaporation => wrong assumption - not all water is evaporated

      % an amount of water evaporated is guessed
      dWguess = acktot/dHevap;
      if dWguess<0
         dWguess=0;
      end
```

```
    % the new boiling point is obtained by a minimization
    % function (fzero)
    options = optimset('Display','off','TolX',1e-15);
    GASES = 0;
    % sum of gas mass (kg)
    for q = 1:7
        GASES = GASES+G(t,x,q);
    end
    [dW, fval, exitflag, output]=...
        fminbnd(@Drying,0,dWguess,options, acktot, W(t,x), ...
        GASES, T(t,x), S(t,x), dHevap, Cps, Cpw,CpE,Cpg, P(t,x));
    % the maximum number of iterations for the boiling point calculation
    % are saved on the variable maxiter here
    if output.iterations > maxiter
        maxiter = output.iterations;
        [maxiter t];
    end
    % the new energy accumulation is reduced
    % as energy is used to evaporate the water
    ack2 = acktot-dW*dHevap;
    % the new water amount is reduced by the amount evaporated
    W(t+1,x) = W(t,x)-dW;
    % the new gas amount is increase by the mass of water evaporated
    G(t+1,x,1) = G(t,x,1) + dW;
else
% All water evaporates
    % dummy value
    ack1 = acktot;
    % maximum amount of water than can be
    % evaporated with the energy in that section
    dW = ack1/dHevap;
    % can't evaporate more water than exists,
    % so the value can't be higher than W(t,x)
    if dW > W(t,x)
        dW = W(t,x);
    end
    % the rest of the energy left to heat up/pyrolyse is calculated
    ack2 = acktot-dW*dHevap;
    % the amount of water in the droplet is reduced by the amount evaporated
    W(t+1,x) = W(t,x)-dW;
    % the amount of gases is increased by the amount of water evaporated
    G(t+1,x,1) = G(t,x,1) + dW;
end
% amounts of solids doesn't change with evaporation of water
S(t+1,x) = S(t,x);
% only water vapour is adding to the accumulated released gases
ARG(t+1) = ARG(t+1)+dW;
% the accumulated water release is increased by the amount evaporated
ACC_GAS(t+1,1) = ACC_GAS(t+1,1) + dW;
% the amount of the 6 other compounds doesn't change during evaporation
for q = 2:7
    G(t+1,x,q) = G(t,x,q);
end
% accumulated evaporated water for each section
H2O_vap(t+1,x) = H2O_vap(t+1,x) + dW;
```

```
% P Y R O L Y S I S

% test for pyrolysis: temperature has to be reached,
% only 40 % can maximally be pyrolysed
% and drying has to be finished
elseif T(t,x) > Tpyro & S(t,x) > 0.6*S0(x) & W(t,x) == 0
   % amount of solids pyrolysed [kg/tstep]
   rpyro=(A1*exp(-E1/Rg/T(t,x))+A2*exp(-E2/Rg/T(t,x)))*S(t,x)/tstep;
   % amount of 4 gases released
   rpyro_gas=0.18425*rpyro;
   % energy accumulation is reduced by the reaction enthalpy
   ack2 = ack(x)-rpyro*dHpyro;
   % the water content is not changed by pyrolysis
   W(t+1,x) = W(t,x);
   % relative amount of pyrolisys gases released (H2O, CO, CO2, CH4, SO2, H2S, N2)
   pyr_comp = [0 0.383 0.552 0.035 0.030 0 0];
   % the gas amount increases for the species involved in pyrolysis
   for q = 2:5
      G(t+1,x,q) = G(t,x,q) + rpyro_gas*pyr_comp(q);
   end
   % no water is released
   G(t+1,x,1) = G(t,x,1);
   % H2S not taken into account (yet) and no N2 released
   G(t+1,x,6) = G(t,x,6);
   G(t+1,x,7) = G(t,x,7);
   % the solids amount decreases by the amount pyrolysed
   S(t+1,x) = S(t,x) - rpyro;
   % the accumulated released gases increase by the amount of pyrolysed solids
   ARG(t+1) = ARG(t+1) + rpyro;
   % the accumulated gas amount is increased
   ACC_GAS(t+1,:) = ACC_GAS(t+1,:) + rpyro_gas*pyr_comp;

% NO EVAPORATION & NO PYROLYSIS
else
   % no changes in water, gas and solid content
   W(t+1,x)=W(t,x);
   G(t+1,x,:)=G(t,x,:);
   S(t+1,x)=S(t,x);
end
% gaseous volume in the section in the beginning
pseudo_gas_start=eps0*V0(x)*Psurr/Rg/Tdrop*M_N2;

% CHANGE IN GAS AMOUNT DUE TO DARCY-FLOW
% outer section
if x == n+1
   if gas_in(x) <= 0
   % gas_in < 0 means gases from section n+1 leave the droplet
      sum_Gas = sum(G(t+1,x,:));
      gas_Detailed(1:7) = gas_in(x)/sum_Gas*G(t+1,x,:);
      % amount of accumulated released gases increases
      for q =1:7
         G(t+1,x,q) = G(t+1,x,q) + gas_Detailed(q);
         Gas_released(t+1,q) = Gas_released(t,q) - gas_Detailed(q);
      end
```

```
    else
    % else N2 will be going in the droplet from the reactor atmosphere
        G(t+1,x,7) = G(t+1,x,7) + gas_in(x);
        % amount of accumulated released gases doesn't increase
        for q = 1:7
            Gas_released(t+1,q) = Gas_released(t,q);
        end
    end
    if gas_out(x) <= 0
    % gas_out < 0 means gases from the inner section (n)
    % will be transported in section n+1
        sum_Gas = sum(G(t+1,x-1,:));
        gas_Detailed(1:7) = gas_out(x)/sum_Gas*G(t+1,x-1,:);
        for q=1:7
            G(t+1,x,q) = G(t+1,x,q) - gas_Detailed(q);
        end
    else
    % gases from section n+1 will move to section n
        sum_Gas = sum(G(t+1,x,:));
        gas_Detailed(1:7) = gas_out(x)/sum_Gas*G(t+1,x,:);
        for q=1:7
            G(t+1,x,q) = G(t+1,x,q) - gas_Detailed(q);
        end
    end

% inner section
elseif x == 1
    if gas_in(x) <= 0
    % means gases from section 1 go to section 2
      sum_Gas = sum(G(t+1,x,:));
      gas_Detailed(1:7) = gas_in(x)/sum_Gas*G(t+1,x,:);
      % amount of gases in section x DECREASED
      for q=1:7
          G(t+1,x,q) = G(t+1,x,q) + gas_Detailed(q);
      end
    else
    % else the gas flowing in will be the one from the outer section
    % (THAT ONLY IS KNOWN FOR TIME t)
      sum_Gas = sum(G(t,x+1,:));
      gas_Detailed(1:7) = gas_in(x)/sum_Gas*G(t,x+1,:);
      % amount of gases in section x INCREASED
      for q=1:7
          G(t+1,x,q) = G(t+1,x,q) + gas_Detailed(q);
      end
    end

% section 2-n
else
    if gas_in(x) <= 0
    % means gases from section x go to section x+1
      sum_Gas = sum(G(t+1,x,:));
      gas_Detailed(1:7) = gas_in(x)/sum_Gas*G(t+1,x,:);
      % amount of gases in section x DECREASED
      for q=1:7
          G(t+1,x,q) = G(t+1,x,q) + gas_Detailed(q);
      end
```

```
    else
    % else the gas flowing in will be the one from the outer section
    % (THAT ONLY IS KNOWN FOR TIME t)
        sum_Gas = sum(G(t,x+1,:));
        gas_Detailed(1:7) = gas_in(x)/sum_Gas*G(t,x+1,:);
        % amount of gases in section x INCREASED
        for q = 1:7
            G(t+1,x,q) = G(t+1,x,q) + gas_Detailed(q);
        end
    end
    if gas_out(x) <= 0
    % means gases from the inner section will move in that section
        sum_Gas = sum(G(t+1,x-1,:));
        gas_Detailed(1:7) = gas_out(x)/sum_Gas*G(t+1,x-1,:);
        % amount of gases in section x INCREASED
        for q = 1:7
            G(t+1,x,q) = G(t+1,x,q) - gas_Detailed(q);
        end
    else
        sum_Gas = sum(G(t+1,x,:));
        gas_Detailed(1:7) = gas_out(x)/sum_Gas*G(t+1,x,:);
        % amount of gases in section x DECREASED
        for q = 1:7
            G(t+1,x,q) = G(t+1,x,q) - gas_Detailed(q);
        end
    end
end  % of Darcy flow calculation

% the rest of the energy is used for heating up the section
dT=ack2/(S(t+1,x)*(Cps+CpE)+W(t+1,x)*(Cpw+CpE)+(sum(G(t+1,x,:))*Cpg));
T(t+1,x)=T(t,x)+dT;
% dummy value for the gas amount
gas_in_volume = sum(G(t+1,x,:));

% SWELLING CALCULATIONS

if gas_in_volume > pseudo_gas_start
%swelling starts
    if x < n+1
    % for all the inner sections
        % new bubble radius calculated by function BLswell
        Rbubnew(x)=BLswell(Pavg1,Rbub(x),Pavg2,tstep,Rbubstart(x), viskbl, St, surfbl);
        % volume increase in cell
        inc=nbub(x)*4*pi/3*(Rbubnew(x)^3-Rbub(x)^3);
        % corresponding radius increase
        drcell=(3/4/pi*(4*pi/3*rinew(x)^3+inc))^(1/3)-rinew(x);
    elseif x==n+1
    % for the outer section
        % new bubble radius calculated by function BLswell
        Rbubnew(x)=BLswell(Pavg,Rbub(x),Psurr,tstep, Rbubstart(x), viskbl, St, surfbl);
        % volume increase in cell
        inc=nbub(x)*4*pi/3*(Rbubnew(x)^3-Rbub(x)^3);
        % corresponding radius increase
        drcell=(3/4/pi*(4*pi/3*rnew(x)^3+inc))^(1/3)-rnew(x);
    end
```

```
            % Recalculation of the section radius and the intersection
            % area radius
            if x==1
               rinew(x)=rinew(x)+drcell;
               rnew(x)=rnew(x);
            elseif x<n+1
               rinew(x)=rinew(x)+drcell;
               rnew(x)=((rinew(x)^3+rinew(x-1)^3)/2)^(1/3);
               for i=x+1:n
                  rinew(i)=(3/4/pi*(4*pi/3*rinew(i-1)^3+V(t,i)))^(1/3);
                  rnew(x)=((rinew(x)^3+rinew(x-1)^3)/2)^(1/3);
               end
               rnew(n+1)=(3/4/pi*(4*pi/3*rinew(n)^3+V(t,n+1)))^(1/3);
            elseif x==n
               rnew(x+1)=(r(t,x)^3-ri(x-1)^3+rinew(x-1)^3)^(1/3);
            else    %x=n+1 in this case
               rnew(x)=rnew(x)+drcell;
            end

            % new volume
            V(t+1,x)=V(t,x)+inc;
            % new porosity
            eps_new(x)=(V(t,x)*eps(t,x)+inc)/V(t+1,x);
            % new average molar mass of gases in section x
            Gas_vector(1:7) = G(t+1,x,:);
            M_avg = Molmass(Gas_vector);
            % new pressure
            P(t+1,x)=gas_in_volume/M_avg*Rg*T(t+1,x)/V(t+1,x)/eps_new(x);

         else
         % no swelling occurs
            % pressure for next time step equal to surrounding pressure
            P(t+1,x) = Psurr;
            % no volume increase
            V(t+1,x) = V(t,x);
         end
         % dummy value for pressure loop
         Pnew(x)=P(t+1,x);
      end     % for x
      % pressure in all sections mustn't change more than the convergence citeria a=0.01
      condition=max(abs(Pguess-Pnew)./Pnew);

      % in case of too high pressure deviations the time step is
      % decreased and the "old" pressure used as guess for a new iteration
      if max(abs(Pguess-P(t,:))) > 5e5
         condition = 1;
         % guessed pressure in the cells at t
         Pguess(1:n+1) = P(t,1:n+1);
         Pnew(1:n+1) = P(t,1:n+1);
         % increase in time step
         tstep = tstep*2;
         a = 0;
      end
   end        % while loop for pressure
```

```
    % porosity, radius, intersection radius and
    % bubble radius for next time step
    eps(t+1,:) = eps_new;
    r(t+1,:) = rnew;
    ri = rinew;
    Rbub = Rbubnew;
    % time vector to keep track of the time steps
    % => possible to step back
    timevec(t+1) = time_s;

end             % while t

% calculating the time needed for the whole calculation (stop watch)
% and displaying it
final_time=toc;
tid1=round(final_time/60);
tid2=round(mod(final_time,60));
total_time=strcat(num2str(tid1),' min :',num2str(tid2),' s');
disp(total_time)
```

Function Molmass.m

```
function Mol_avg = Molmass(Gas)

% ==========================================
% CALCULATION FOR 7 COMPOUNDS
% calculates the average molar mass of the gas mixture
% "Gas" is a vector with all the masses of the different
% gas components in the following order:
% 1) H2O
% 2) CO
% 3) CO2
% 4) CH4
% 5) SO2
% 6) H2S
% 7) N2
% ==========================================
M(1) = 0.018;   % [kg/mol]
M(2) = 0.028;   % [kg/mol]
M(3) = 0.044;   % [kg/mol]
M(4) = 0.016;   % [kg/mol]
M(5) = 0.064;   % [kg/mol]
M(6) = 0.034;   % [kg/mol]
M(7) = 0.028;   % [kg/mol]
% overall number of moles
ntot = sum(Gas./M);
% vector with the molar fraction of each component
Y = (Gas./M)./ntot;
% average molar mass as sum of mole fraction times molar mass
Mol_avg = sum(Y.*M);
```

Function heatcap.m

```
function [Cpw, Cps, CpE]=heatcap(Temp,Solid)

% calculates the heat capacities based on temperature and solid content
% temp = temperature in Kelvin
% Solid = dry content of black liquor

% heat capacity of water (assumed constant)
Cpw = 4180;   % [J/kg,K]
% temperature in degree celcius
T = Temp-273; % [deg C]
% heat capacity of solids
Cps = 1684 + 4.47*T; % [J/kg,K]
% excess heat capacity
CpE = (4930 - 29*T)*(1 - Solid)*Solid^3.2; % [J/kg,K]
```

Function drying.m

```
function Tboil=Drying(dW, acktot, Wold, Gold, Told, Sold, dHevap, Cps, Cpw,CpE, Cpg,
Pressure)

% function to determine the boiling point during evaporation
% using the minimization algorithm fminbnd
% (constrained minimization of a function of one variable)
% variable to be optimized: dW = evaporated water

% energy left after evaporation
ack2=acktot-dW*dHevap;
% new water content
Wnew=Wold-dW;
% new gas amount
Gnew=Gold+dW;
% heating up of the section with the energy left
dT=ack2/(Sold*(Cps+CpE)+Wnew*(Cpw+CpE)+Gnew*Cpg);
% new temperature
Tnew=Told+dT;
% dry content
St=Sold/(Sold+Wnew);
% new boiling point
Tboilnew=373.15+50*St.^2.74+101.06*(Pressure/1e5)^0.2487-101.39;

% difference between calculated new temperature and new boiling point
% to be minimized, when equal to 0, amount of water evaporated is correct
Tboil=Tnew-Tboilnew;
```

Function BLswell.m

```
function Rb = BLswell(Pbub,Rbub0,Psurr,tstep, bubstart, visk, Dc, surfbl)

% function to determine the swelling of the bubbles
% in one section of the black liquor droplet depending
% on the pressure

% radius increase per time dRdt [m/s]
dRdtcal1 = Rbub0*(Pbub-Psurr)/visk;
dRdtcal2 = 2*surfbl/visk;
dRdtcal = dRdtcal1-dRdtcal2;
dRdt=dRdtcal;

% new bubbble radius [m]
Rb = Rbub0+dRdt/tstep;

% the bubble radius is not allowed to get smaller
% than the initial radius
if Rb < bubstart
   Rb=bubstart;
end
```

Appendix B – Optimization program code

Optimization for the case of 4 parameters (2 reactions) at 375 °C and an optimization based on the measured CO release.

Main program optim_first.m

```
% ====================================
% OPTIMIZATION OF KINETIC PARAMETERS WITH FMINSEARCH
% ====================================
clear all

global data data1 d0 rho change_factor CO2_measured CO_measured CH4_measured
global SO2_measured time time_vect T_profile dHypro Tpyro Rg T_profile_exp
global tstep S0 CO_calculated S_shell CO_calculated_all residual

%Input data
Tpyro = 273+300;  % temperature of pyrolysis onset (K)
Rg = 8.3145;      % gas constant (J/mol,K)
dHpyro = 1.45e5;  % heat of reaction [J/kg BLS]
d0 = 4.2e-3;      % droplet diameter
rho = 1200;       % black liquor density
tstep = 2;        % time steps (1/s) - calculations done every 0.5 seconds only

% Accessing of data file
channel_1 = ddeinit('excel','Matlab_375.xls');
% four columns: CO, CO2, CH4 and SO2 accumulated amount [kg]
data = str2num(strrep(ddereq(channel_1,'r3c20:r703c23',[1 1]),',','.'));
% average T-profile from experiments (1 column)
data1 = str2num(strrep(ddereq(channel_1,'r3c7:r703c7',[1 1]),',','.'));

% relating measured data (for 1 mg to value used for simulations) to
% simulation value
% mg - to change values to the amount of BL used in the simulation
change_factor = pi/6*d0^3*rho*10^6;
CO2_measured = (data(:,1).*change_factor)';
CO_measured = (data(:,2).*change_factor)';
CH4_measured = (data(:,3).*change_factor)';
SO2_measured = (data(:,4).*change_factor)';
T_profile_exp = data1+273;

time = [0:0.5:350];

% getting the temperature profile, initial solids mass and timevector
load 375_DC64.mat T
load 375_DC64.mat S0
load 375_DC64.mat timevec
```

```
% picking the values of the calculated temperature profile at values 0,
% 0.5, 1, 1.5 ... seconds
time_vect = timevec;
T_profile(1,:) = T(1,:);
for i = 2:length(time)
   T_profile(i,:) = T(find(time_vect == (i-1)/2),:);
end

% defining the mass of each section
S_shell(1:11) = S0;

% giving starting values
A1_start = 3.7e5;
E1_start = 7.36e4;
A2_start = 1.46e13;
E2_start = 2.51e5;

% starting guess vector
guess = [A1_start, E1_start, A2_start,E2_start];
% setting the options for the optimization
options = optimset('fminsearch');
options = optimset(options,'TolFun',1e-60,'TolX',1e-30,'MaxFunEvals',1e3);
% optimization function
[x, Fval,exitflag,output] = fminsearch(@first_step,guess,options,CO_measured,time,T_profile);

% result output
exitflag
disp('Starting guess A1: '),disp(guess(1));
disp('Starting guess E1: '), disp(guess(2));
disp('Starting guess A2: '), disp(guess(3));
disp('Starting guess E2: '), disp(guess(4));
disp('Final value A1: '), disp(x(1));
disp('Final value E1: '), disp(x(2));
disp('Final value A2: '), disp(x(3));
disp('Final value E2: '), disp(x(4));
```

Optimization function first_step.m

```
% objective function to be minimized

function residual = first_step(guess,CO_measured,time,T_profile)

global CO_calculated S0 tstep Tpyro Rg S_shell CO_calculated_all residual

% using the values as kinetic parameters
A1 =guess(1);
E1 =guess(2);
A2 =guess(3);
E2 =guess(4);
```

```
% the programme is calculating the CO_release in the 11 sections every
% 0.5 seconds and adding all up in the end to compare it to the accumulated
% amount from the experiments

t = 1;
S(1,:) = S_shell;
CO_calculated(1,1:11) = 0;

for t=1:length(time) % calculations every 0.5 seconds
   % P Y R O L Y S I S
   for i = 1:11 % each section
      % Pyrolysis start temperature has to be reached
      % and only a certain amount of solids can be
      % pyrolysed (value from experiments)
      if T_profile(t,i) > Tpyro & S(t,i) > 0.6*S_shell(i)
         % relative amount of pyrolisys gases released (H2O, CO, CO2, CH4, SO2, H2S, N2)
         pyr_comp = [0 0.383 0.552 0.035 0.030 0 0];
         % amount of solids pyrolysed
         rpyro=(A1*exp(-E1/Rg/T_profile(t,i))+A2*exp(-E2/Rg/T_profile(t,i)))*S(t,i)/tstep;
         % only about 7.5% of all solids are converted to the four gases
         rpyro_gas = 0.180925*rpyro;
         % accumulated amount of CO released for each section
         CO_calculated(t+1,i) = CO_calculated(t,i) + rpyro_gas*pyr_comp(2);
         % the solids amount decreases by the amount pyrolysed
         S(t+1,i) = S(t,i) - rpyro;
      % NO EVAPORATION & NO PYROLYSIS
      else
         S(t+1,i)=S(t,i);
         CO_calculated(t+1,i) = CO_calculated(t,i);
      end
   end % for i
   % summing up the CO release for a time over all sections
   CO_calculated_all(t) = sum(CO_calculated(t,:));
end   % for t

% calculating the difference for each time between
% measured and calculated value
for i = 1:length(time)
   difference(i) = CO_measured(i)-CO_calculated_all(i);
end

% display residual sum of squares during iterations
disp(sum(difference.^2));

% Objective function value
residual=(sum(difference.^2))/10^-6;
```